

Old Dominion University

ODU Digital Commons

Electrical & Computer Engineering Theses &
Dissertations

Electrical & Computer Engineering

Spring 2013

Impact of Primary User Activity on the Performance of Energy-Based Spectrum Sensing in Cognitive Radio Systems

Sara L. MacDonald
Old Dominion University

Follow this and additional works at: https://digitalcommons.odu.edu/ece_etds



Part of the [Digital Communications and Networking Commons](#), [Power and Energy Commons](#), [Signal Processing Commons](#), [Systems and Communications Commons](#), and the [Theory and Algorithms Commons](#)

Recommended Citation

MacDonald, Sara L.. "Impact of Primary User Activity on the Performance of Energy-Based Spectrum Sensing in Cognitive Radio Systems" (2013). Master of Science (MS), Thesis, Electrical & Computer Engineering, Old Dominion University, DOI: 10.25777/ngtf-nt17
https://digitalcommons.odu.edu/ece_etds/430

This Thesis is brought to you for free and open access by the Electrical & Computer Engineering at ODU Digital Commons. It has been accepted for inclusion in Electrical & Computer Engineering Theses & Dissertations by an authorized administrator of ODU Digital Commons. For more information, please contact digitalcommons@odu.edu.

**IMPACT OF PRIMARY USER ACTIVITY ON THE
PERFORMANCE OF ENERGY-BASED SPECTRUM SENSING IN
COGNITIVE RADIO SYSTEMS**

by

Sara L. MacDonald

B.S. May 2000, South Dakota School of Mines and Technology

A Thesis Submitted to the Faculty of
Old Dominion University in Partial Fulfillment of the
Requirements for the Degree of

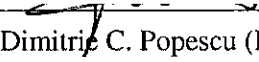
MASTER OF SCIENCE

ELECTRICAL AND COMPUTER ENGINEERING

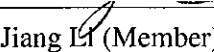
OLD DOMINION UNIVERSITY

May 2013

Approved by:


Dimitrie C. Popescu (Director)


W. Steven Gray (Member)


Jiang Li (Member)

ABSTRACT

IMPACT OF PRIMARY USER ACTIVITY ON THE PERFORMANCE OF ENERGY-BASED SPECTRUM SENSING IN COGNITIVE RADIO SYSTEMS

Sara L. MacDonald
Old Dominion University, 2013
Director: Dr. Dimitrie C. Popescu

Increasing numbers of wireless devices and mobile data requirements have led to a spectrum shortage. However spectrum utilization percentages are often low due to the current static spectrum allocation process where primary users (PUs) are given exclusive use to spectrum. Several mechanisms to increase spectrum utilization have been proposed including opportunistic spectrum access (OSA). Cognitive Radio (CR) is an emerging concept in wireless communication systems that aims to enable OSA in licensed frequencies by secondary users (SUs). CR systems are expected to sense the spectrum in order to determine if the PU is transmitting. Therefore OSA performance relies on the ability of the SU to accurately sense the spectrum and detect the PU activity. Numerous approaches have been studied for spectrum sensing; one of the most common is energy-based detection due to the SU needing no prior knowledge of the PU waveform. While energy detection has been widely studied, the assumption has been made that the PU status, either ON or OFF, does not change while the SU is actively sensing the spectrum. The work presented in this thesis examines specifically the impact to performance of energy detectors when the PU status changes during the spectrum sensing period. Two alternative analytic expressions for the probabilities of detection and false alarm are derived and corroborated with numerical results obtained from simulations. While the work presented in this thesis is discussed in terms of SU spectrum sensing performance, the analytic expressions apply to all applications in which energy detection is used.

ACKNOWLEDGEMENTS

I would like to acknowledge and express my gratitude to my advisor, Dr. Dimitrie C. Popescu. His guidance, support, and encouragement were key in the completion of my graduate work. In addition to being my advisor, I had the privilege of taking two courses from him, both of which I learned a great deal and thoroughly enjoyed. His knowledge and enthusiasm has provided me motivation to strive for technical excellence. Further, I appreciate his patience and flexibility which has allowed me to pursue my career and educational goals simultaneously.

I would like to thank Dr. W. Steven Gray and Dr. Jiang Li for serving on my thesis committee. I would not have been able to complete the work presented within this thesis if it were not for the thorough manner in which they instructed related courses. I asked them to serve as committee members because of the great respect I have for their technical abilities and am grateful they accepted.

I would like to thank MITRE for funding my education. Additionally I would like to thank my supervisors and colleagues at MITRE for their flexibility which has allowed me to attend on-campus classes.

Finally I would like to thank my parents for instilling in me the importance of education, my husband for being so supportive of my goals, Tiffany for reminding me of what is truly important in life, and Rusty for being the sweetest little boy in the world.

TABLE OF CONTENTS

	Page
LIST OF FIGURES	vi
Chapter	
1. INTRODUCTION.....	1
1.1 COGNITIVE RADIO SYSTEMS.....	1
1.2 OPPORTUNISTIC SPECTRUM ACCESS	3
1.3 SPECTRUM SENSING TECHNIQUES	5
1.4 SPECTRUM SENSING PERFORMANCE MEASURES	7
1.5 PROBLEM STATEMENT	9
1.6 THESIS OUTLINE.....	10
2. ENERGY DETECTION	12
2.1 THE ENERGY DETECTOR	12
2.2 ENERGY DETECTION IN A DYNAMIC SCENARIO	14
3. SPECTRUM SENSING IN DYNAMIC SCENARIOS	17
3.1 PROBABILITY OF DYNAMIC PRIMARY USER STATE SWITCH	17
3.2 DYNAMIC PRIMARY USER IMPACT ON SENSING PERFORMANCE ..	20
3.3 DYNAMIC PRIMARY USER NUMERICAL EXAMPLES	24
4. EXTENSION TO VOLATILE SCENARIOS.....	30
4.1 PROBABILITY OF VOLATILE PRIMARY USER STATE SWITCH	30
4.2 VOLATILE PRIMARY USER IMPACT ON SENSING PERFORMANCE ..	37
4.3 VOLATILE PRIMARY USER NUMERICAL RESULTS	38
5. CONCLUSIONS.....	43

REFERENCES 44

VITA 48

LIST OF FIGURES

Figure	Page
1. Dynamic spectrum access techniques.....	4
2. Potential OSA dimensions.....	5
3. Example receiver operating characteristic curve.....	8
4. Example of probability of error versus λ	9
5. Basic energy detector block diagram.	13
6. Sensing spectrum holes with finite duration in discrete time domain.	15
7. Switching during observation period.	17
8. P_s versus N for varying PU activity levels.	20
9. Dynamic PU sensing window probabilities versus N for $\mu=100$, $\tau=10$	21
10. Dynamic PU sensing window probabilities versus N for $\mu=100$, $\tau=100$	21
11. Dynamic PU sensing window probabilities versus N for $\mu=100$, $\tau=200$	22
12. Dynamic PU ROCs for $\mu=100$, $\tau=10$, and $\gamma = -5$ dB.....	26
13. Dynamic PU ROCs for $\mu=100$, $\tau=10$, and $\gamma = 0$ dB.	26
14. Dynamic PU ROCs for $\mu=100$, $\tau=100$, and $\gamma = -5$ dB.	27
15. Dynamic PU ROCs for $\mu=100$, $\tau=100$, and $\gamma = 0$ dB.	27
16. Dynamic PU ROCs for $\mu=100$, $\tau=200$, and $\gamma = -5$ dB.	28
17. Dynamic PU ROCs for $\mu=100$, $\tau=100$, and $\gamma = 0$ dB.	28

18.	Higher order PU switching during sensing window.	31
19.	Markov chain representation of PU activity.	32
20.	Volatile PU sensing window probabilities versus N for $\mu=100, \tau=10$	35
21.	Volatile PU sensing window probabilities versus N for $\mu=100, \tau=100$	36
22.	Volatile PU sensing window probabilities versus N for $\mu=100, \tau=200$	36
23.	Volatile PU ROCs for $\mu=100, \tau=10$, and $\gamma = -5$ dB.	40
24.	Volatile PU ROCs for $\mu=100, \tau=10$, and $\gamma = 0$ dB.	40
25.	Volatile PU ROCs for $\mu=100, \tau=100$, and $\gamma = -5$ dB.	41
26.	Volatile PU ROCs for $\mu=100, \tau=100$, and $\gamma = 0$ dB.	41
27.	Volatile PU ROCs for $\mu=100, \tau=200$, and $\gamma = -5$ dB.	42
28.	Volatile PU ROCs for $\mu=100, \tau=100$, and $\gamma = 0$ dB.	42

CHAPTER 1

INTRODUCTION

The RF spectrum in the United States and other parts of the world appears to be overcrowded. The ever growing bandwidth demands of commercial and military users have made spectrum a shortage. Wireless devices are growing in number and in data rate requirements. It is increasingly the case where the hardware is no longer the limiting factor in the achievable data rate of a wireless device, but instead spectrum availability.

According to measurements taken by the FCC's Spectrum Policy Task Force, spectrum utilization ranges geographically and temporally from 15% to 85% [1]. Ideally, the duty cycle would be much higher, but the current spectrum allocation policy provides exclusive rights to the spectrum holder. If the spectrum holder is not using the frequency, it remains idle. Therefore, the apparent spectrum shortage is partially an artifact of the current spectrum policy. In unlicensed bands where there is no spectrum holder, the duty cycle is very high. Because wireless devices have equal access to the spectrum in unlicensed bands, techniques have been implemented to share spectrum and ensure spectral efficiency and the highest achievable data rates.

There are further policy reasons for exploring spectrum sharing. The White House has backed FCC plans to make 500 MHz of government and commercial spectrum available for auction [2]. The goal of the reallocation is to get 500 MHz more spectrum in the hands of wireless broadband providers over the next decade as part of the FCC's National Broadband Plan. While 500 MHz will help, it likely will not be adequate using conventional static allocation techniques. Additionally, due to the expense of moving current government systems to new frequency bands, the President's Council of Advisors on Science and Technology (PCAST) report recently recommended sharing of spectrum rather than reallocation [3]. Therefore, exploring methods to successfully share spectrum is of importance.

1.1 COGNITIVE RADIO SYSTEMS

Cognitive Radio (CR) is an emerging concept that is expected to contribute to spectrum sharing and more efficient use of the frequency spectrum in future generations of wireless systems by enabling dynamic spectrum access (DSA) [4]. While there are many variations on the definition of a CR, the FCCs definition has been widely adopted:

“Cognitive Radio: A radio or system that senses its operational electromagnetic environment and can dynamically and autonomously adjust its radio operating parameters to modify system operation, such as maximize throughput, mitigate interference, facilitate interoperability, access secondary markets.” [1].

Using this definition of CR, techniques for detecting the radio environment is clearly a key component of CR technology. However, CR is a broad interdisciplinary topic, involving spectral analysis, control systems, computer networking, game theory, and formal languages, amongst other technical disciplines [5].

Dr. Joseph Mitola III led the research and development in the area of CR. His early work in software-defined radios led to his concept of CR. Mitola’s vision of CR was more robust than the FCCs definition. He first described software-defined radios that were fully aware of not only spectrum availability, but other aspects of the communication system [6]. Between 2002 and 2005, Mitola served as Special Assistant to the Director of the Defense Advanced Research Projects Agency (DARPA) to develop the Next Generation (XG) and Wireless Network after Next (WNaN) programs. DARPA’s XG and WNaN programs focused on the development of low cost military handheld terminals that utilize CR techniques. The WNaN military radios are capable of sensing spectrum, opportunistically utilizing unused spectrum, and dynamically shifting utilized spectrum to optimize spectrum utilization across the entire channel.

Outside of military applications, there are several commercial applications that make use of CR. In the 2.4 and 5.725 GHz unlicensed bands, several devices are beginning to implement CR technology. IEEE 802.11k is an update to the WLAN standard that includes spectrum sensing to help determine which access point a WLAN device should connect

to. Additionally, Bluetooth now includes Adaptive Frequency Hopping (AFH) as a way of reducing interference with the numerous other devices operating in this band. AFH senses which portions of the band are busy and does not transmit on those frequencies. This reduces interference and thus increases performance for both the Bluetooth device and other wireless devices operating in the band.

An additional commercial application of CR is the work being done by the IEEE 802.22 Working Group on Wireless Regional Area Networks (WRAN). IEEE802.22 has a goal of developing a standard for unlicensed access to white spaces in UHF TV bands (400-800 MHz). The FCC indicates that in most geographical areas there are multiple unused 6 MHz channels. Because of the long range propagation characteristics in this band, the aim of this technology is to provide wireless broadband access in rural areas.

1.2 OPPORTUNISTIC SPECTRUM ACCESS

Several DSA techniques have been proposed to increase utilization of available spectrum over the current static allocation method. DSA techniques fall into three subcategories; dynamic exclusive use model, open sharing model, and hierarchical access model as shown in Figure 1. One of the subcategories of the hierarchical access model, opportunistic spectrum access (OSA) has received a lot of attention because it is believed to be achievable with little impact on legacy systems operating within the current static spectrum allocation system.

OSA is a technology that is within the realm of CR. As indicated in Figure 1, OSA is a form of hierarchical access. It is hierarchical in the sense that there are primary and secondary users to given frequency spectrum. The assignment of spectrum to primary users (PUs) is generally assumed to be static much like the current spectrum allocation system. It is also assumed that the PU will access the spectrum in the same manner, or similar to, the current method. That is, the PU will transmit without consideration of potential interference to secondary users (SUs). On the other hand, the SUs will only access spectrum if the transmission will not interfere with PUs.

There are multiple dimensions in which SUs may transmit without interfering with the PU as shown in Figure 2 and described below. SUs may take advantage of spectrum

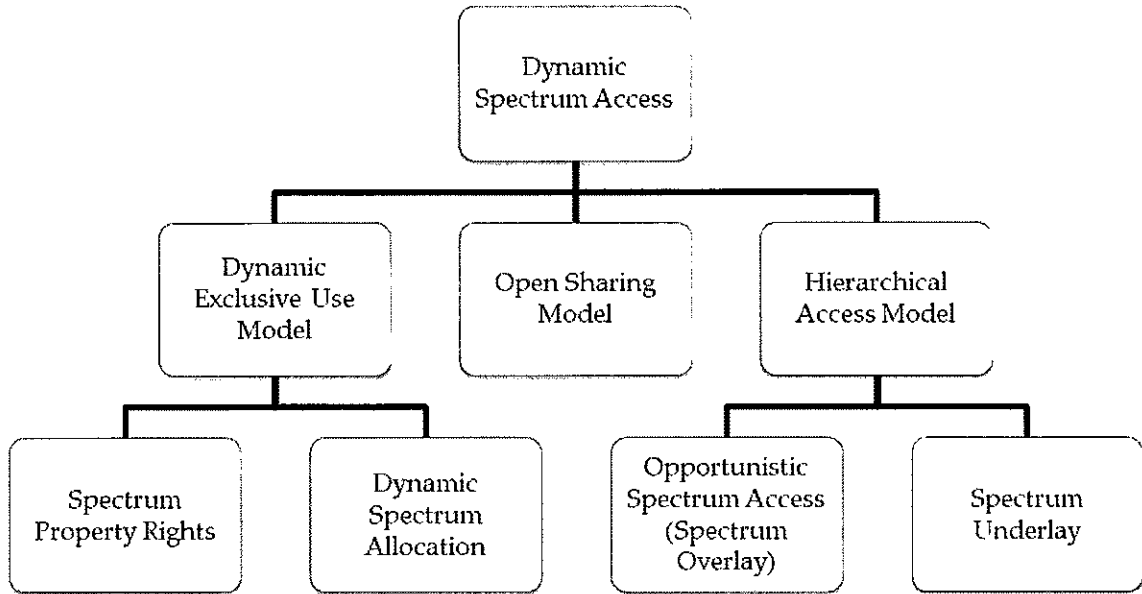


Figure 1: Dynamic spectrum access techniques.

opportunities, or spectrum holes, in one or more of these dimensions.

A. Frequency: If the spectrum allocation is broken into multiple narrow bands of spectrum, some of these smaller bands may go unused by the PU. These smaller bands of spectrum could potentially be used by SUs. The UHF TV bands are an extreme example of opportunities within the frequency domain. In the case of UHF TV bands these opportunities are relatively static over time, so they can be exploited with negligible impact to PUs.

B. Time: If the PU is not transmitting constantly, there are periods when the spectrum is idle and a SU could access the spectrum. Because network loading generally varies greatly over time, certain times of the day may have extended opportunities in the time domain while others may have relatively few opportunities.

C. Geospatial: If a SU is an adequate distance from the PU, then that SU may be able

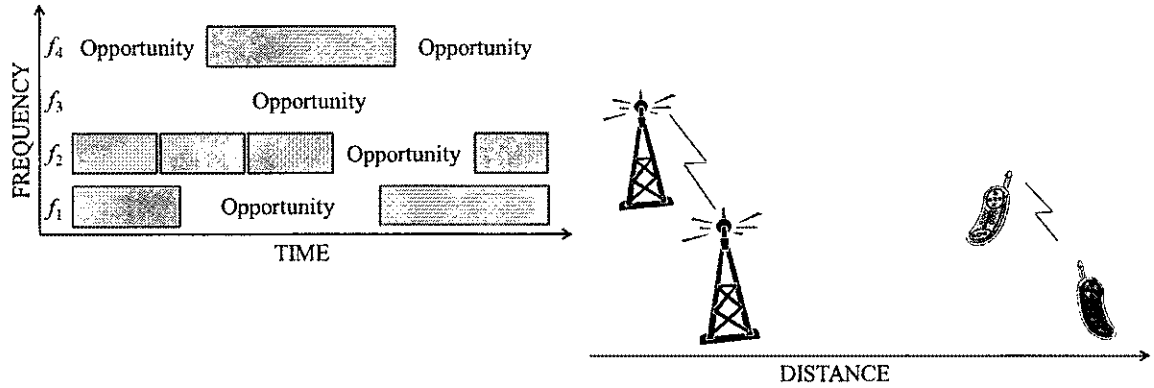


Figure 2: Potential OSA dimensions.

to transmit without interfering with the PUs transmission. Geospatial separation can also take advantage of directional transmissions and often relies on power control of the SU.

It is critical within OSA that the SU causes minimal interference to the PU. OSA is therefore reliant on the SU ability to accurately sense spectrum occupancy by the PU. The following section provides an overview of spectrum sensing.

1.3 SPECTRUM SENSING TECHNIQUES

Spectrum sensing is the general term used to describe methods in which SUs sense PU transmissions. The objective of spectrum sensing is for the SU to decide between the two hypotheses:

$$H_0 : r(n) = u(n) \quad (1)$$

$$H_1 : r(n) = s(n) + u(n), \quad (2)$$

where $r(n)$ is the received signal, $u(n)$ is the noise, and $s(n)$ is the signal transmitted by the PUs. Many approaches to spectrum sensing have been identified. These techniques range in complexity and accuracy. The most popular of these approaches are summarized in the following sections.

1.3.1 ENERGY DETECTION

The most basic and most common form of spectrum sensing is energy detection. It requires no knowledge of the PU's waveform so it is more universal than other forms of spectrum sensing. However, it is less accurate and does not work with CDMA systems [7]. An energy detector will compare the power spectral density (PSD) of the received signal to a threshold level λ . The value of λ is critical as it determines the success of the opportunity identification using the probabilities [8]

$$P_d = P\{|r(t)|^2 > \lambda|H_1\} \quad (3)$$

$$P_f = P\{|r(t)|^2 > \lambda|H_0\}, \quad (4)$$

where P_d is the probability of successfully detecting a transmitted signal and P_f is the probability of a false alarm. A detailed discussion of energy detection follows in Chapter 2.

1.3.2 WAVEFORM-BASED SENSING

Also called coherent sensing, this method requires knowledge of the PU's waveform. It utilizes preambles, spreading sequences, and other patterns. These pilot patterns allow the waveform to be detected by correlating the received signal with a copy of itself. Using the same hypothesis in (1) and (2), the values of P_d and P_f are [9]

$$P_d = P\{r(t)s^*(t) > \lambda|H_1\} \quad (5)$$

$$P_f = P\{r(t)s^*(t) > \lambda|H_0\}. \quad (6)$$

Just as in energy detection, setting the threshold level λ is critical to the performance of the both the primary and secondary users.

1.3.3 CYCLOSTATIONARY SENSING

Also called feature detection, cyclostationary sensing does not use the power spectral density of the receive signal but instead uses a cyclic correlation function. Cyclostationary detection is capable of differentiating noise from the transmitted signal. This is possible because AWGN is wide sense stationary with no correlation and transmitted signals are

typically spectrally correlated. Cyclostationary sensing uses a spectral correlation density (SCD) function [10],

$$S(f, \alpha) = \sum_{-\infty}^{\infty} R_y^\alpha e^{-j2\pi f\tau} \quad (7)$$

where

$$R_y^\alpha = E[y(n + \tau)y^*(n - \tau)e^{-j2\pi f\tau}]. \quad (8)$$

Therefore the decision probabilities are

$$P_d = P\{S(f, \alpha) > \lambda | H_1\} \quad (9)$$

$$P_f = P\{S(f, \alpha) > \lambda | H_0\}. \quad (10)$$

1.3.4 MATCHED FILTER

A matched filter requires demodulation of the PUs signal. This equates to knowledge of the PUs media access schema, frame formatting, modulation technique, pulse shaping, etc. With matched-filtering a certain P_d or P_f can be achieved with relatively few samples, although the rate at which this is achieved is waveform dependent [11]. It is the most accurate of the mentioned schema. However, it is considered somewhat impractical because of power constraints and hardware requirements to demodulate the signal of all potential PU waveforms.

1.4 SPECTRUM SENSING PERFORMANCE MEASURES

If a spectral hole or opportunity has been identified after sensing the spectrum, the SU then determines whether to exploit the opportunity. This decision is multifaceted and must be determined by sharing information collaboratively between the media access control (MAC) and physical (PHY)-layers. Additionally the decision to exploit the spectrum hole may be based on the number of SUs in the area, the number of PUs in the area, the MAC layer performance and techniques, and the channel condition. Finally, opportunity exploitation will depend largely on regulatory policy which will define the tolerable impact

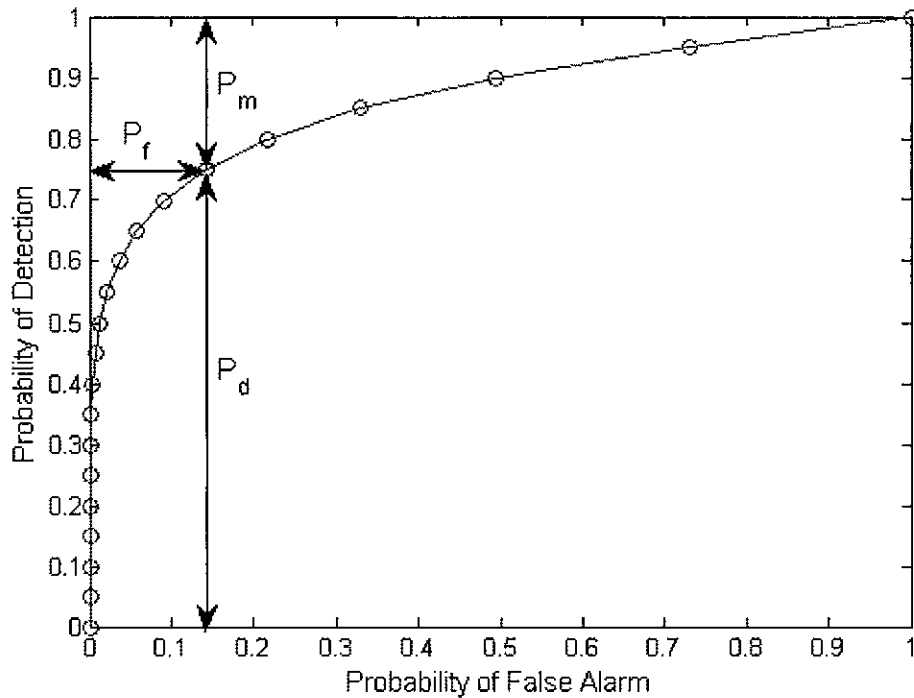


Figure 3: Example receiver operating characteristic curve.

or the PU. Spectrum sensing performance measures are utilized to examine the impact on the PU.

When examining spectrum sensing performance, the two probabilities discussed in the prior section are of concern. The first is the probability of detection, P_d , which is the probability of the SU accurately detecting the PU. The other probability of concern is the probability of false alarm, P_f , or the probability of the SU falsely determining that the PU is active. These values are often plotted against each other in a receiver operating characteristic (ROC) curve. Figure 3 provides an example ROC curve.

The spectrum sensing techniques described are dependent on the threshold value λ . Different values of λ will result in different points on the ROC curve. If λ is set too large then the probability of false alarm will also be high resulting in missed opportunities to access the spectrum. However if λ is set too low then the probability of missed identification, $P_m = 1 - P_d$, will be high. A high P_m value could result in interference to the PUs.

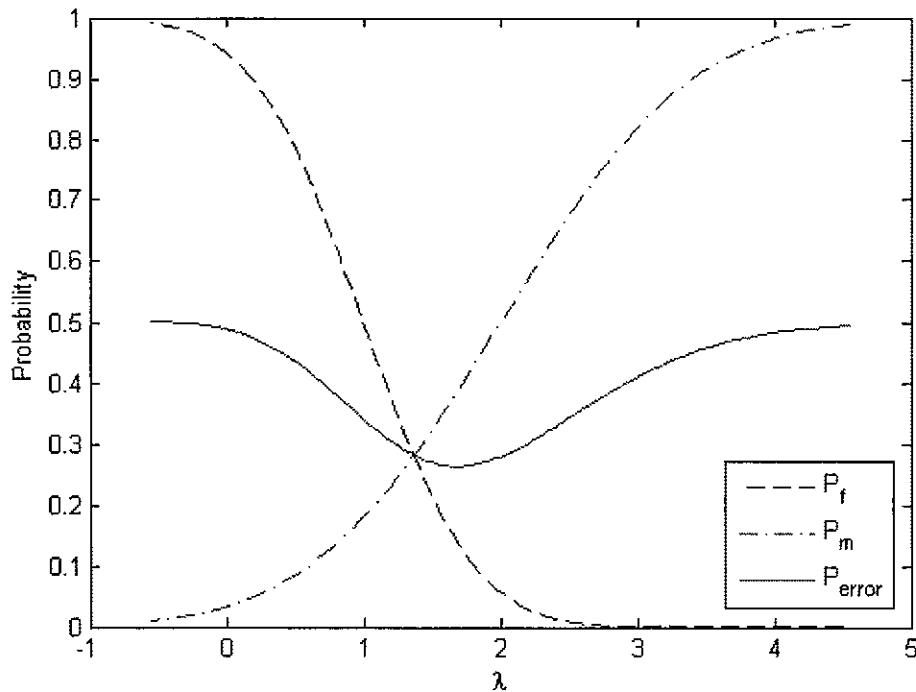


Figure 4: Example of probability of error versus λ .

In addition to utilizing ROC curves, spectrum sensing performance is often evaluated based on the probability of error P_{error} which is described as

$$P_{error} = \alpha \cdot P_m + (1 - \alpha) \cdot P_f. \quad (11)$$

where α is a weighing factor which determines the weight of the individual contributions. Figure 1.4 illustrates an example P_{error} versus λ where α is set to 0.5. Examining sensing performance in this manner facilitates the selection of the proper threshold value of λ .

1.5 PROBLEM STATEMENT

In order to increase spectrum utilization, it is desirable to explore spectrum sharing techniques. CR through the use of OSA offers an avenue for spectrum sharing. However, OSA is reliant on spectrum sensing techniques. Numerous approaches have been studied for spectrum sensing, among which the most common ones are based on energy detection, matched filtering, waveform-based sensing, or cyclostationarity [12]. Each is suitable for

different scenarios dependent on the SU knowledge of the PU waveform and the processing capability of the SU. This thesis considers a SU with no knowledge of the PU waveform. Therefore energy detection is a suitable technique. Commonly cited analytic expressions have been derived which quantify the performance of energy based detectors [8], [13], and [14]. However, these analytic expressions are obtained under the assumption that the PU signal does not change state during the spectrum sensing period in which the SU is making its determination as to whether the spectrum is available or not. This is a restrictive assumption that limits the applicability of the analytic expressions.

The work presented in this thesis considers energy-based spectrum sensing in dynamic CR systems where PU transmissions occur at random time instances and have limited durations [15]. These result in spectrum holes [16] with finite duration determined by the PU activity, that must be accurately detected by SU for OSA. Further, this work assumes that the PU signal may change while the SU senses the spectrum. The performance of the energy detector is studied in terms of the probabilities of detection P_d and false alarm P_f . Specifically, two alternative expressions for P_d and P_f are derived which explicitly include the probability of the PU signal switching state while the SU senses the spectrum P_s . The value of P_s is determined based on the dynamic activity of the PU described by the average duration of PU transmissions, the average duration of spectrum holes, and the length of the SU sensing window.

1.6 THESIS OUTLINE

This thesis is organized by first providing an overview of prior research and then detailing the contributions of this thesis. Chapter 2 provides energy detection analytic expressions which have been previously studied under the assumption that the PU does not switch states during the SU sensing period. Commonly cited energy detection performance metrics are provided. Chapter 3 and 4 contain the original contribution of this thesis. Chapter 3 derives analytic energy detection performance metrics which explicitly consider the probability that a PU switches states while the SU is actively sensing the spectrum. The work in Chapter 3 assumes that the PU switches states a single time while the SU is sensing the spectrum. Chapter 4 removes this assumption and provides alternative analytic expressions

for energy detection performance. Conclusions are provided in Chapter 5.

The original work described within this thesis has been submitted for inclusion in IEEE Globecom 2013 conference proceedings.

CHAPTER 2

ENERGY DETECTION

In this work a SU is considered with no a priori knowledge of the PU waveform or transmission timing. Energy-based spectrum sensing is a suitable technique when SUs have no knowledge of the PU signals. Energy detection has been studied in various scenarios [17–22]. This chapter first provides detail of the energy detection model and provides the derivation of commonly utilized analytic expressions for energy-based detection and its performance. This chapter then outlines a dynamic energy detection scenario in which the aforementioned analytic expressions for energy-based detection and its performance require modification.

2.1 THE ENERGY DETECTOR

The spectrum sensing and energy detection model are described following the work in [14]. The PU signal received at the SU is

$$r(n) = s(n) + u(n), \quad (12)$$

where the PU signal $s(n)$ is a real-valued, zero-mean iid random process with signal variance σ_s^2 . The noise $u(n)$ is a real-valued Gaussian, iid process with zero-mean and variance σ_u^2 . Therefore the signal-to-noise ratio (SNR) is $\gamma = \sigma_s^2/\sigma_u^2$. Further, when the PU signal is absent, the signal received at the SU is

$$r(n) = u(n). \quad (13)$$

The role of the energy detector is to determine between two hypothesis H_1 and H_0 or the presence or absence of the PU respectively. As illustrated in Figure 5, this is done by squaring the sampled received signals and integrating them over the sensing window T where $N = Tf_s$ samples represent the received samples within the sensing window. The

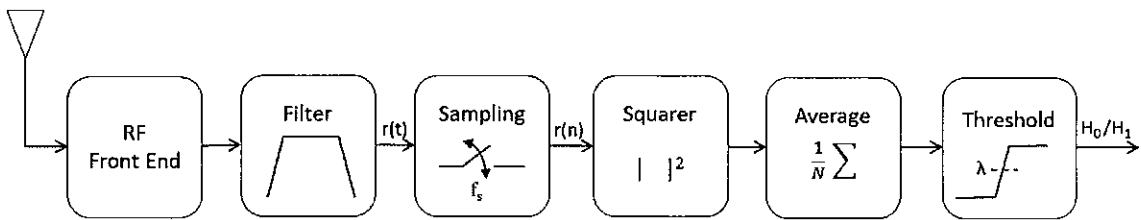


Figure 5: Basic energy detector block diagram.

average of the N samples is compared to the threshold value λ to formulate a hypothesis. Therefore the test statistic for distinguishing between the two hypotheses H_0 and H_1 which corresponds to energy detection is:

$$Y(N) = \frac{1}{N} \sum_{n=1}^N |r(n)|^2 \underset{H_0}{\overset{H_1}{\geq}} \lambda. \quad (14)$$

Under the assumption that the PU state (either ON or OFF) is constant for the entire sensing window the test statistic $Y(N)$ follows a chi-squared distribution

$$Y(N) \sim \begin{cases} \chi_N^2, & \text{for } H_0 \\ \chi_N^2(\gamma), & \text{for } H_1, \end{cases} \quad (15)$$

where χ_N^2 and $\chi_N^2(\gamma)$ denote the central and non-central chi-squared distributions with N degrees of freedom and a non-centrality parameter of γ in the case of H_1 [8]. The output of the integrator $Y(N)$ is compared to a threshold value, λ and the result of this comparison provides a hypothesis as to whether the PUs signal is present or not. In a non-fading environment, the probability of false alarm and detection using the N samples received in observation window T is shown in [23] to be

$$P_f(N) = \Pr(Y > \lambda | H_0) = \int_{\lambda}^{\infty} \chi_N^2 dr = \frac{\Gamma(N, \lambda/2)}{\Gamma(N)} \quad (16)$$

$$P_d(N) = \Pr(Y > \lambda | H_1) = \int_{\lambda}^{\infty} \chi_N^2(\gamma) dr = Q_M(\sqrt{2\gamma}, \sqrt{\lambda}). \quad (17)$$

where $\Gamma(\cdot)$ and $\Gamma(\cdot, \cdot)$ are complete and incomplete gamma functions, respectively, and $Q_M(\cdot, \cdot)$ is the generalized Marcum Q -function.

When N is large, the central limit theorem may be applied thus simplifying the expressions. The tail regions of the chi-squared distributions corresponding to the test statistic in (15) larger than the threshold $Y(N) > \lambda$ may be approximated by corresponding tails of normal distributions [14]:

$$Y(N) \sim \begin{cases} \mathcal{N}(\sigma_u^2, \frac{2}{N}\sigma_u^4), & \text{for } H_0 \\ \mathcal{N}((1+\gamma)\sigma_u^2, \frac{2}{N}\sigma_u^4(1+2\gamma)\sigma_u^4), & \text{for } H_1. \end{cases} \quad (18)$$

This implies that the probabilities of false alarm and detection may be computed using the standard Q -function as [14]

$$P_f(N) = \Pr(Y > \lambda | H_0) = Q\left(\frac{\lambda - \sigma_u^2}{\sigma_u^2 \sqrt{2/N}}\right) \quad (19)$$

$$P_d(N) = \Pr(Y > \lambda | H_1) = Q\left(\frac{\lambda - (1+\gamma)\sigma_u^2}{\sigma_u^2 \sqrt{2(1+2\gamma)/N}}\right). \quad (20)$$

P_f is independent of γ since in the case of H_0 there is no primary signal present. However, P_d is dependent on γ , and as shown in [24], is hence dependent on the channel fading conditions. Therefore, in the presence of fading, 17 becomes

$$P_d(T) = \int_x Q(\sqrt{2\gamma}, \sqrt{\lambda}) f_\gamma(x) dx, \quad (21)$$

where $f_\gamma(x)$ is the probability distribution function of the γ under fading. In the case of Rayleigh fading, γ has an exponential distribution, and P_d is shown in [24] to be

$$P_d(T) = e^{-\frac{\lambda}{2}} \sum_{n=0}^{N-2} \frac{1}{n!} \left(\frac{\lambda}{2}\right)^n + \left(\frac{1+\bar{\gamma}}{\bar{\gamma}}\right)^{N-1} \times \left(e^{-\frac{\lambda}{2(1+\bar{\gamma})}} - e^{-\frac{\lambda}{2}} \sum_{n=0}^{N-2} \frac{1}{n!} \left(\frac{\lambda\bar{\gamma}}{2(1+\bar{\gamma})}\right)^n\right), \quad (22)$$

where $\bar{\gamma}$ is the mean value of γ .

2.2 ENERGY DETECTION IN A DYNAMIC SCENARIO

The dynamic energy detection scenario considers a single SU. The SU employs CR for OSA to a licensed spectrum band where a PU signal switches ON and OFF at random time instances with random transmission and spectral hole durations. The SU samples the received signal at a sampling rate of f_s over the sensing window of length T . The

SU determines its hypothesis, H_0 or H_1 , based on the samples collected over the sensing window. The total number of samples collected over the sensing window is $N = T f_s$. This scenario is illustrated in Figure 6.

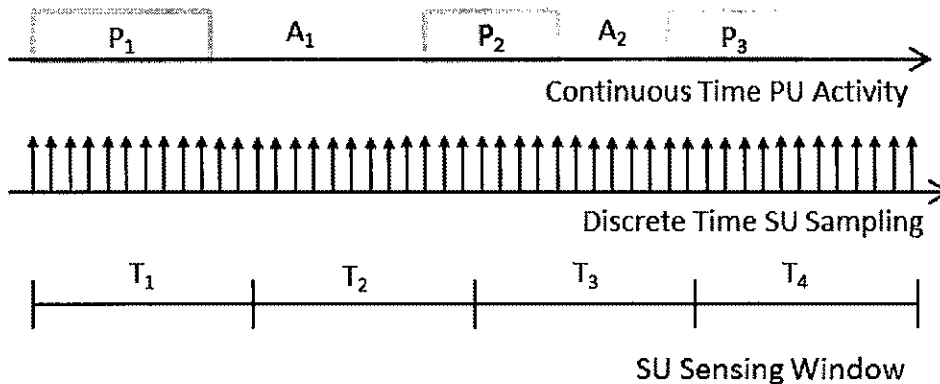


Figure 6: Sensing spectrum holes with finite duration in discrete time domain.

The sequence of PU transmissions (PU signal is present/ON) and spectrum holes (PU signal is absent/OFF) are respectively represented in Figure 6 by $\{\mathcal{P}_i\}$ and $\{\mathcal{A}_i\}$. These correspond to mutually exclusive states of the spectrum as the occurrence of a PU transmission \mathcal{P}_i implies the absence of a spectrum hole \mathcal{A}_i and vice versa. The duration of a spectrum hole \mathcal{A}_i and that of a PU transmission \mathcal{P}_i are exponentially distributed with means μ and τ , respectively [25]. For convenience, μ and τ are defined from the perspective of the SU. Therefore, in the context of discrete time processing by the SU where signals are sampled with some sampling frequency f_s , the values of μ and τ represent the average number of samples corresponding to PU transmissions and spectrum holes. Thus, the continuous time duration of a spectrum hole \mathcal{A}_i and that of a PU transmission \mathcal{P}_i have means μ/f_s and τ/f_s , respectively.

The analytic expressions in the prior section do not appropriately capture the performance of a system when the PU changes states within an SU sensing window. The next two chapters will extend the energy detection performance metrics such that the expressions are inclusive of the dynamic scenario described. It is noted that discontinuous PU signals are described in [22, 26], but the corresponding analysis is presented in a static context. Furthermore [21] considers a dynamic PU which may switch states between the end of the

sensing window and the time when the SU exploits the perceived spectrum hole. However, the probability of the PU switching states during the sensing window is not considered.

CHAPTER 3

SPECTRUM SENSING IN DYNAMIC SCENARIOS

The expressions for the probabilities of detection and false alarm provided in the prior chapter were obtained under the assumption that the PU state does not change during the sensing window. However, this is a restrictive assumption that limits the applicability of the derived expressions in a dynamic scenario where the PU transmission timing is not known to the SU. Thus, the PU state may change while calculation of the spectrum sensing test statistic is in progress. In this chapter the activity of the PU is explicitly considered. The average durations of PU transmissions and spectrum holes are used to determine a probability of PU state switch P_s during a sensing window of duration T . Furthermore, analytic expressions which consider the influence of P_s on the energy detection performance metrics P_d and P_f are derived. This chapter is concluded with numerical results which corroborate the proposed analytic expressions.

3.1 PROBABILITY OF DYNAMIC PRIMARY USER STATE SWITCH

Again, the work presented in this thesis considers energy-based spectrum sensing in dynamic CR systems where PU transmissions occur at random time instances and have limited durations [17]. Consider the example shown in Figure 7 which illustrates a possible scenario of PU activity over four consecutive sampling windows, labeled T_1 through T_4 :

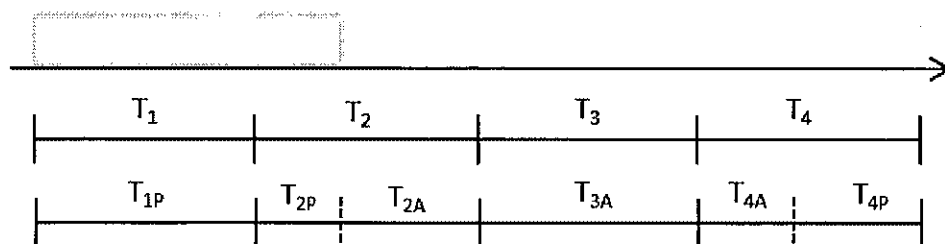


Figure 7: Switching during observation period.

As seen from Figure 7, the four sensing windows shown may be subdivided into non-overlapping intervals corresponding to PU state ON (or present denoted by the subscript P):

T_{1P} , T_{3P} , and T_{4P}), respectively intervals corresponding to PU state OFF (or absent denoted by the subscript A : T_{2A} , T_{3A} , and T_{4A}). Within Figure 7 four cases are distinguished: T_1 in which the PU state is ON for the entire window, T_2 where the PU state switches from ON to OFF, T_3 in which the PU state is OFF the entire window, and T_4 where the PU state switches from OFF to ON. The probabilities of each of these cases occurring in any given sensing window are defined as P_{ON} , $P_{ON \rightarrow OFF}$, P_{OFF} , and $P_{OFF \rightarrow ON}$.

To evaluate the four sensing window probabilities, first observe that the four cases are mutually exclusive, thus their probabilities add to unity. Second, it is noted that each case is dependent on both the state of the PU at the beginning of the sensing window and the PU activity during the sensing window. In the context of the dynamic scenario described in Chapter 2 and illustrated in Figure 6, the probability of the PU being present (ON) at the beginning of a sensing window (or at any time instant) is

$$p_p = \frac{\tau}{\tau + \mu}, \quad (23)$$

while the probability of the PU being absent (OFF) is

$$p_a = \frac{\mu}{\tau + \mu}. \quad (24)$$

The PU activity during the sensing window captures the probability of the PU switching (or not switching) in N samples and is derived from the exponential probability distribution function. The PU state and the PU switching behavior are independent. Therefore, the probability of each type of sensing window occurring is defined as the joint probability of two independent probabilities. Beginning with P_{ON} , the probability of the PU being ON for the duration of a sensing window is the joint probability of the PU being present and the probability the PU does not switch during within N samples, namely,

$$P_{ON} = p_p \cdot e^{-N/\tau}. \quad (25)$$

Similarly, the probability of the PU switching ON to OFF within a sensing window is the joint probability of the PU being present and the PU switching within N samples,

$$P_{ON \rightarrow OFF} = p_p \cdot (1 - e^{-N/\tau}). \quad (26)$$

It is noted that the latter part of this expression represents the probability of the PU switching one or more times during the sensing window. It is assumed however that the probability of higher order PU switching, i.e., more than once in a sensing window, is negligible. Therefore, this expression is used under the limiting assumption that if the PU is ON at the beginning of the sensing window and switches during that sensing window, the PU will be OFF at the end of the sensing window. The work presented in the next chapter will remove this limitation. The probability of the PU remaining OFF for the duration of a sensing window is the joint probability of the PU being absent and the PU not switching within N samples,

$$P_{OFF} = p_a \cdot e^{-N/\mu}. \quad (27)$$

Finally, the probability of the PU switching OFF to ON within a sensing window is the joint probability of the PU being absent and the PU switching within N samples,

$$P_{OFF \rightarrow ON} = p_a \cdot (1 - e^{-N/\mu}). \quad (28)$$

Again, this expression is used under the limiting assumption that probability of higher order PU state switching during a sensing window is negligible.

While not used explicitly in further calculations, it is informative to define an overall probability of PU switching (either ON to OFF or from OFF to ON) during a sensing window as:

$$\begin{aligned} P_s(N) &= P_{ON \rightarrow OFF} + P_{OFF \rightarrow ON} \\ &= \frac{\tau}{\tau + \mu} (1 - e^{-N/\tau}) + \frac{\mu}{\tau + \mu} (1 - e^{-N/\mu}). \end{aligned} \quad (29)$$

Figure 8 illustrates the dependence of the PU state switch during a sensing window P_s on the size of the sensing window N for different patterns of the PU activity given by the average values τ and μ . It is noted that P_s increases with N as the longer the sensing window is the more chances there are for a dynamic PU to switch states. It is also noted that for a given size of the spectrum sensing window, P_s increases when the activity of the PU is more dynamic, as implied by a smaller τ value.

Figures 9, 10, and 11 provide the individual switching window probabilities versus N for the three PU activity levels: $\tau = 10$ and $\mu = 100$, $\tau = 100$ and $\mu = 100$, and $\tau = 200$

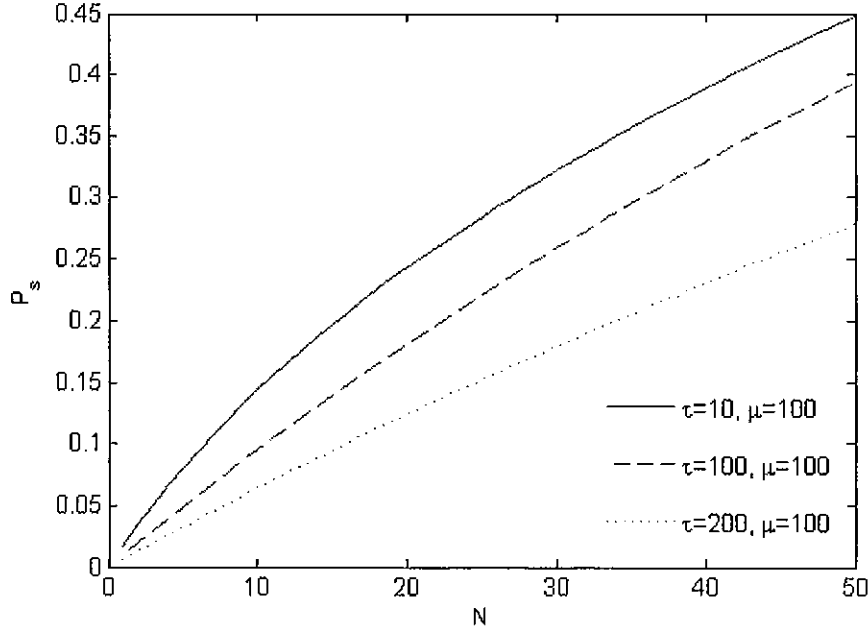


Figure 8: P_s versus N for varying PU activity levels.

and $\mu = 100$. It is noted that in all three figures the sum of the sensing window probabilities adds to unity for each value of N . Examining the figures independently reveals further items of interest concerning the three PU activity levels.

Figure 9 illustrates the switching probabilities for PU activity level $\tau = 10$ and $\mu = 100$. Of interest are the probabilities which contribute to P_s . $P_{OFF \rightarrow ON}$ is the major contributor to P_s while $P_{ON \rightarrow OFF}$ is upper bounded by p_p , in this case 9.1%. In fact $P_{OFF \rightarrow ON}$ also upper bounded, but by p_a , which is equal to 90.9%. Therefore, $P_{OFF \rightarrow ON}$ does not approach its upper bound until approximately $N = 400$. Furthermore, Figure 9 illustrates P_{ON} is negligible for larger values of N .

As one would expect, equal values of μ and τ result in P_{ON} and P_{OFF} being equal and $P_{ON \rightarrow OFF}$ and $P_{OFF \rightarrow ON}$ being equal. This is shown in Figure 10 for a PU activity level of $\tau = 100$ and $\mu = 100$.

When examining Figure 11 which illustrates the PU activity level $\tau = 200$ and $\mu = 100$, it is noted that the values of $P_{ON \rightarrow OFF}$ and $P_{OFF \rightarrow ON}$ closely track one another until N is approximately 30. This is despite the value τ being twice as large as μ .

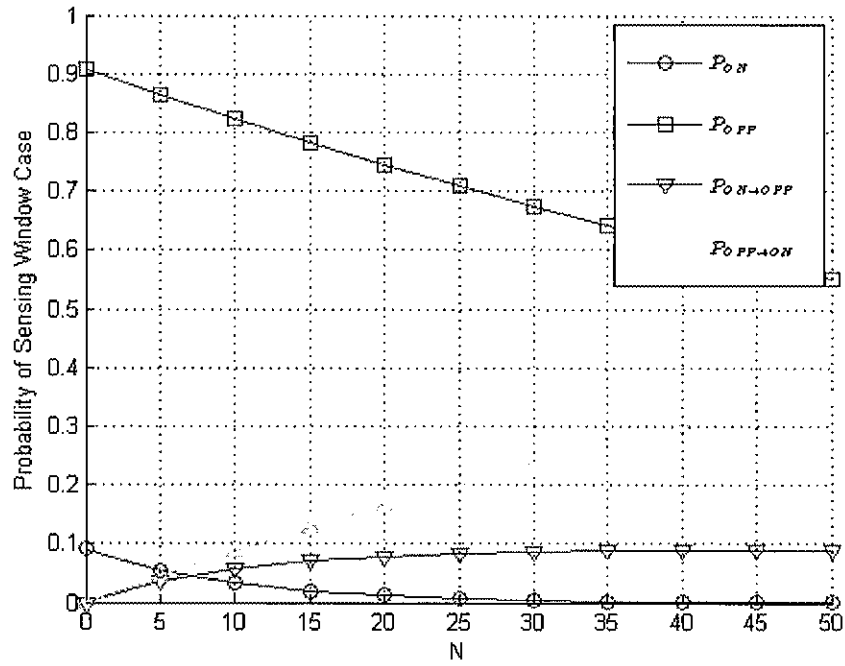


Figure 9: Dynamic PU sensing window probabilities versus N for $\mu=100$, $\tau=10$.

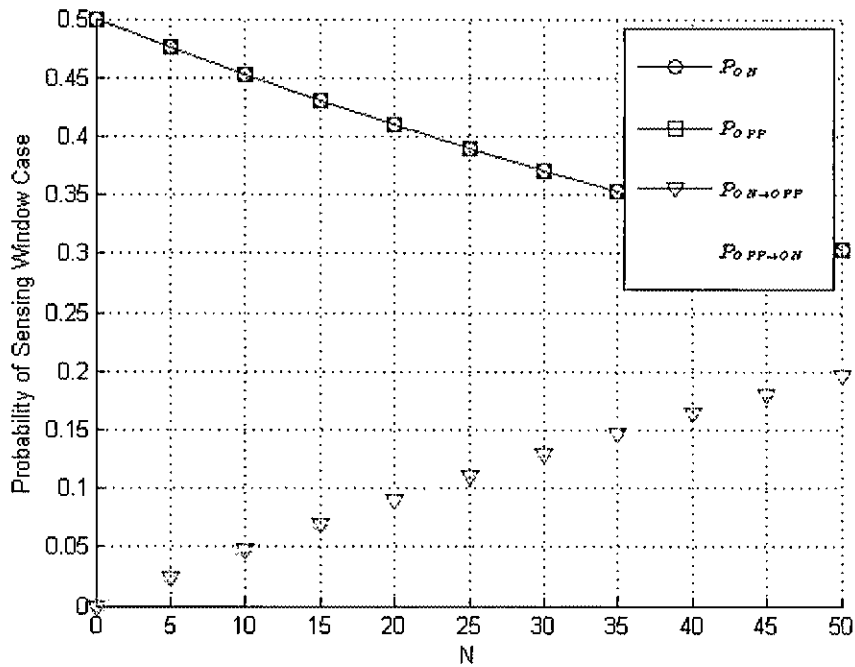


Figure 10: Dynamic PU sensing window probabilities versus N for $\mu=100$, $\tau=100$.

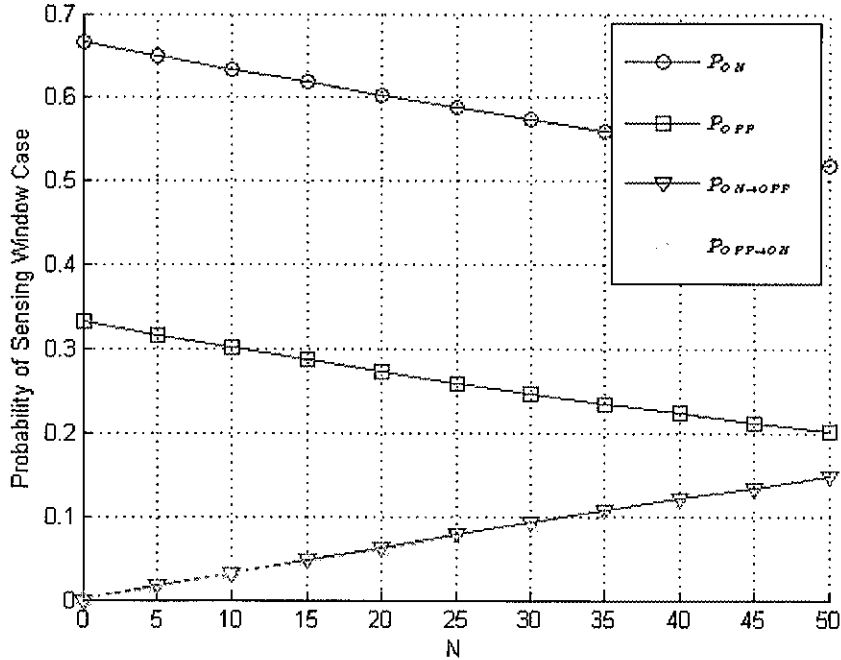


Figure 11: Dynamic PU sensing window probabilities versus N for $\mu=100$, $\tau=200$.

3.2 DYNAMIC PRIMARY USER IMPACT ON SENSING PERFORMANCE

In order to evaluate the impact of the PU state switch on the performance of the SU spectrum sensing it is first recognized that the definitions of the probabilities of detection and false alarm given in Chapter 2, equations (16) and (17), are no longer accurate when the state of the PU switches while spectrum sensing is performed. Specifically, in the context of OSA, sensing is performed to determine if the spectrum is available for use at the completion of the sensing window. Thus, the probabilities of detection and false alarm should be redefined by comparing the test statistic $Y(N)$ in (15) to the threshold λ given that the state of the PU at the end of the sensing window corresponds to a specific hypothesis, that is

$$P'_d(N) = \Pr(Y > \lambda | H_1 \text{ is true at time instant } N) \quad (30)$$

$$P'_f(N) = \Pr(Y > \lambda | H_0 \text{ is true at time instant } N). \quad (31)$$

It is noted that in [22] the probabilities of false alarm and detection were also redefined

to consider PU switching. However within [22] this is done using alternate hypotheses H_{free} and H_{busy} that correspond to the PU absent during the spectrum sensing window, respectively present at any point during the spectrum sensing window.

To determine the expression for the probability of detection that factors in the impact of the PU state switch, one should consider both the case where the PU is ON for the entire sensing window and the case where the PU switches from OFF to ON at some point during the sensing window. These cases are illustrated by the sensing windows T_1 and T_4 in Figure 7 and represented by the probabilities P_{ON} in equation (25) and $P_{OFF \rightarrow ON}$ in equation (28). According to the new definition of the probability of detection (30), only the cases where the PU is present at the end of the sensing window should be considered, and thus, the other two cases are not considered. Furthermore, when the PU state is ON for the entire sensing window the probability of detection is $P_d(N)$ as outlined in Chapter 2 and is given by either (17) in the case of AWGN channels or (21) for fading channels. Whereas when the PU state switches from OFF to ON, the probability of detection $P_{ds}(N)$ is given by

$$P_{ds}(N) = p_p \cdot P_d(N_P) + p_a \cdot P_f(N_A) \quad (32)$$

where $N_P = N \cdot p_p$, $N_A = N \cdot p_a$, $P_d(N_P)$ is the probability of detection corresponding to a sensing window size N_p and no PU switch, and $P_f(N_A)$ is the probability of false alarm corresponding to a sensing window of size N_a and no PU switch. This is illustrated in Figure 7 where the sampling window T_4 is subdivided into sampling windows T_{4A} and T_{4P} . Thus, the expression of the probability of detection that considers the PU state switch is:

$$P'_d(N) = \frac{P_{ON} \cdot P_d(N) + P_{OFF \rightarrow ON} \cdot P_{ds}(N)}{P_{ON} + P_{OFF \rightarrow ON}}. \quad (33)$$

To determine the expression for the probability of false alarm that takes into account the impact of the PU state switch, a similar analysis is carried out. In this case one should consider the case where the PU is OFF for the entire sensing window along with the case where the PU switches from ON to OFF during the sensing window. When the PU state is OFF for the entire sensing window the probability of false alarm is $P_f(N)$ as outlined in Chapter 2 and is given by (16), while when the PU state switches from ON to OFF, the

probability of false alarm $P_{fs}(N)$ is

$$P_{fs}(N) = p_p \cdot P_d(N_P) + p_a \cdot P_f(N_A), \quad (34)$$

where N_P , N_A , $P_d(N_P)$, and $P_f(N_A)$ have the same meaning as in the previous case. It is noted that expression (34) for P_{fs} and expression (32) for P_{ds} are equivalent. Thus, the expression for the probability of false alarm that considers the PU state switch is

$$P'_f(N) = \frac{P_{OFF} \cdot P_f(N) + P_{ON \rightarrow OFF} \cdot P_{fs}(N)}{P_{OFF} + P_{ON \rightarrow OFF}}. \quad (35)$$

3.3 DYNAMIC PRIMARY USER NUMERICAL EXAMPLES

This section presents simulated results which are compared to the theoretical ROC expressions from Chapter 2, which do not consider P_s , and the proposed theoretical ROC expressions within this chapter, which considers P_s . The results illustrate the performance of the proposed expressions. The simulation considered the varying PU activity levels represented in Figure 8. The PU activity was simulated for a period equivalent to 100,000 samples. The SU sampled the received signal in consecutive sensing windows of size N . As shown in Figure 6, the SU sensing windows are independent of the PU activity. In each simulation the number of samples N was selected to yield optimal ROC performance.

The threshold value of λ was calculated using target values of P_d in a non-fading environment using (20). Each simulation used target values of P_d between 69% and 99%. The same threshold values were used within the AWGN and Rayleigh channels, which accounts for theoretical P_d values for Rayleigh fading channels being less than 69%.

AWGN and Rayleigh fading channels were analyzed. The theoretical ROC which considers P_s used the expressions for P'_d and P'_f in this chapter, respectively equation (33) and (35), where P_d and P_f used in the expressions are respectively (22) and (19) for Rayleigh fading channels and respectively (20) and (19) for AWGN channels. The theoretical ROC which does not consider P_s uses equations (22) and (19) for Rayleigh channels and (20) and (19) for AWGN channels. Finally, for each of the PU activity levels two SNR values, $\gamma = -5$ dB and $\gamma = 0$ dB, were simulated.

The first two simulations examined an average PU signal duration which was small relative to the average hole duration, i.e., $p_p < p_a$. The PU activity level represented by

$\tau = 10$ and $\mu = 100$ was examined first with a $\gamma = -5$ dB with results in Figure 12. With $N = 35$ and $\tau = 10$ the value of P_s is particularly high. As illustrated, the simulated results are a far better fit to the ROC which considers P_s for both the AWGN and Rayleigh fading channels. Of interest, there is little difference between the AWGN and Rayleigh fading channels in both the simulated results and the theoretical ROC which considers P_s . This can be attributed to P'_d being dominated by the case $P_{OFF \rightarrow ON}$ in which the probability of detection is determined by P_{ds} in (32). Furthermore, when p_a is much larger than p_p , as is the case with this PU activity level, the value of P_{ds} is dominated by P_f . As noted in Chapter 2, P_f is independent of the communication channel thus the two channels have similar performance.

The second simulation used the same PU activity level as the first but γ was increased to 0 dB. The results of the second simulation are provided in Figure 13. The higher SNR allowed for a smaller sensing window with $N = 17$ thus reducing P_s . While the simulated values are a better fit to the theoretical ROC in which P_s was considered, neither of the theoretical expressions are truly representative of the simulated results.

The next two simulations considered a PU activity level in which p_p was equal to p_a . The PU activity level represented by $\tau = 100$ and $\mu = 100$ was examined first with a $\gamma = -5$ dB with results in Figure 14 then with $\gamma = 0$ dB with results in Figure 15. Both simulations yielded results that closely matched the curve of the theoretical ROC in which P_s was considered, however, the points on the curve are shifted indicating that the theoretical expressions for P'_d and P'_f are slightly optimistic in this case.

The final two simulations considered a PU activity level in which the average PU signal duration was larger than the average hole duration. The PU activity level represented by $\tau = 200$ and $\mu = 100$ was first simulated with $\gamma = -5$ dB with results in Figure 16 then with $\gamma = 0$ dB with results in Figure 17. Both simulations yielded results that were a relatively close match to the theoretical ROC in which P_s was considered. Again, the simulation values are aligned well the theoretical ROC in which P_s was considered, but the individual points were shifted on the curve.

In this chapter, the impact of PU activity level on the overall sensing performance of an energy detector was examined. The simulation results indicate that in the context of the

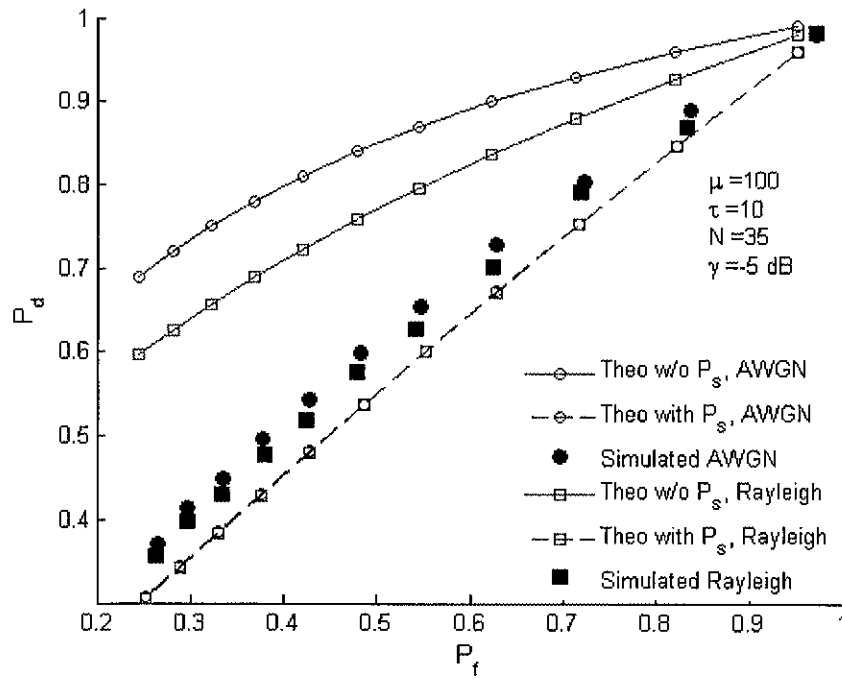


Figure 12: Dynamic PU ROCs for $\mu=100$, $\tau=10$, and $\gamma = -5$ dB.

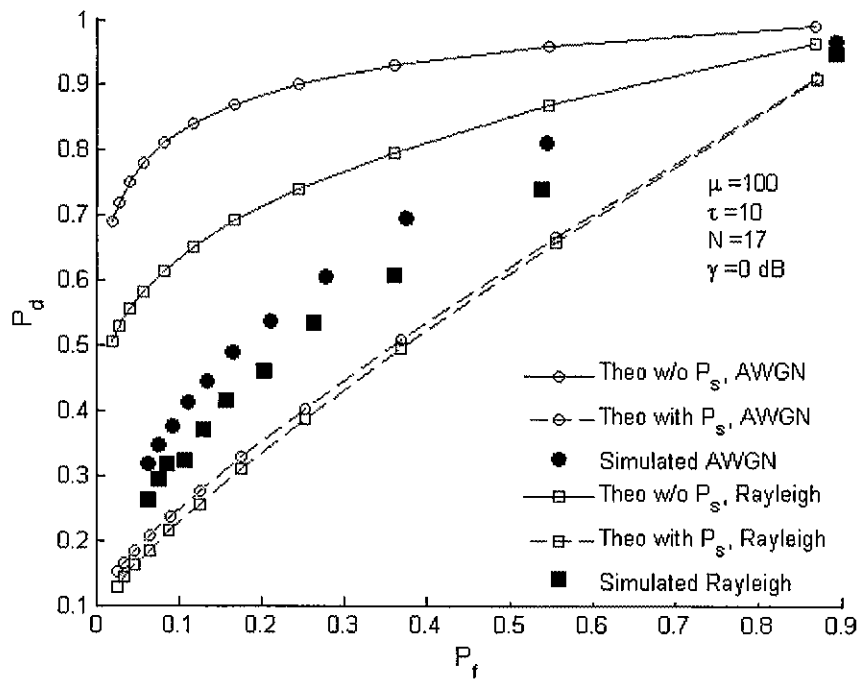


Figure 13: Dynamic PU ROCs for $\mu=100$, $\tau=10$, and $\gamma = 0$ dB.

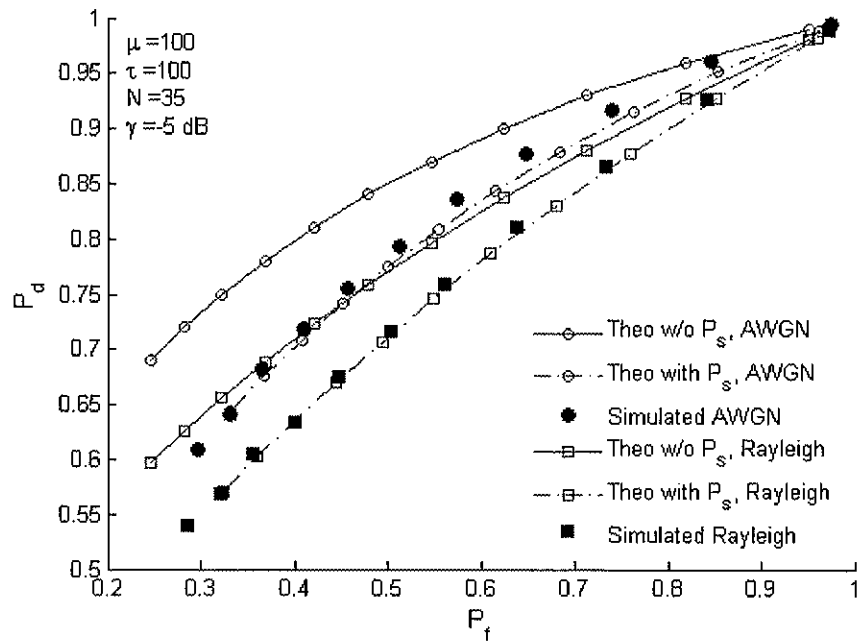


Figure 14: Dynamic PU ROCs for $\mu=100$, $\tau=100$, and $\gamma = -5$ dB.

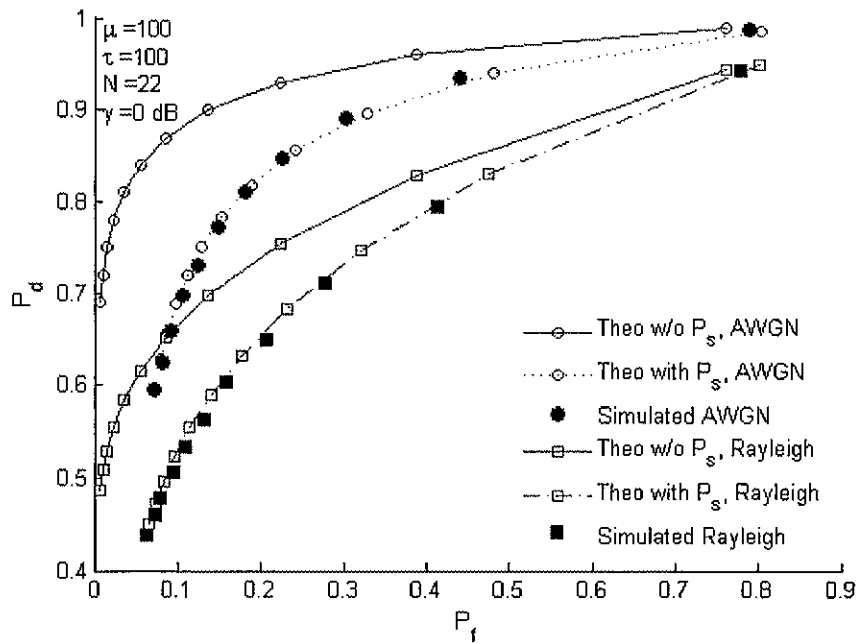


Figure 15: Dynamic PU ROCs for $\mu=100$, $\tau=100$, and $\gamma = 0$ dB.

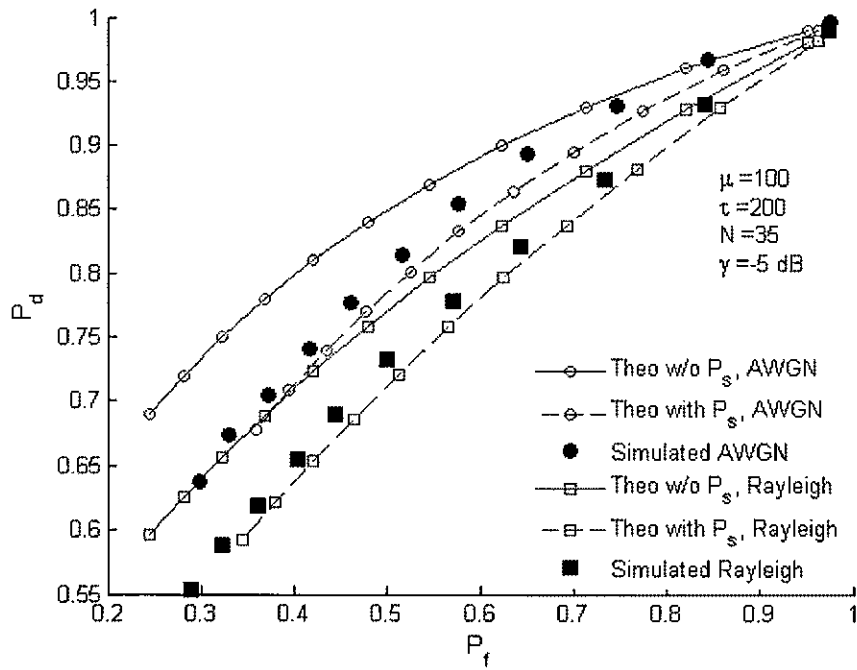


Figure 16: Dynamic PU ROCs for $\mu=100$, $\tau=200$, and $\gamma = -5$ dB.

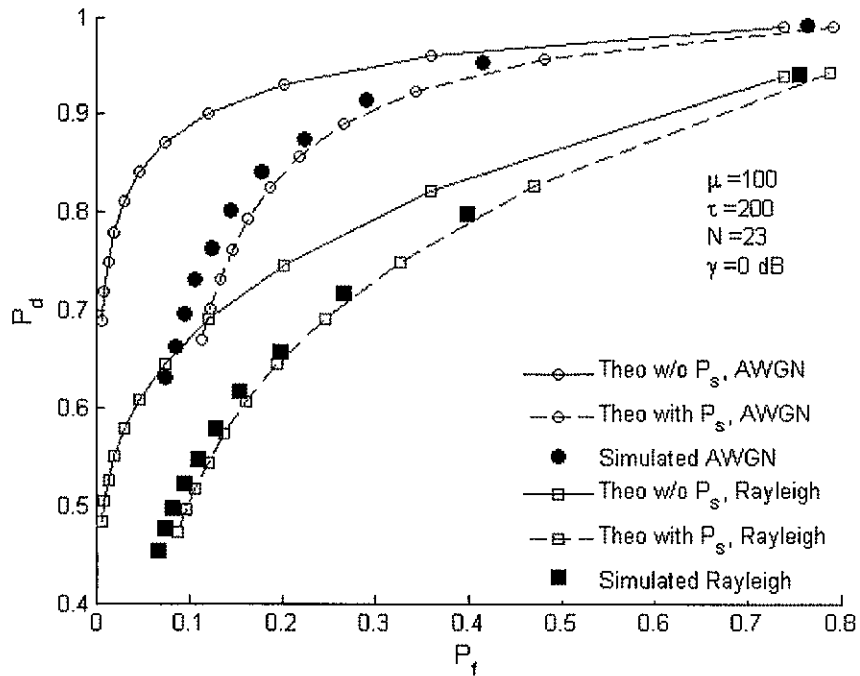


Figure 17: Dynamic PU ROCs for $\mu=100$, $\tau=100$, and $\gamma = 0$ dB.

dynamic scenario described in Chapter 2, the proposed expressions for P'_d and P'_f within this chapter are a better analytical measure of performance than the values of P_d and P_f given in Chapter 2. However, the values of P'_d and P'_f consider a single PU state switch within the sensing window; OFF to ON in the calculation of P'_d and ON to OFF in the case of P'_f . While this limitation is likely adequate for most PU activity levels, the next chapter considers instances of higher order PU switching.

CHAPTER 4

EXTENSION TO VOLATILE SCENARIOS

The probability of the PU switching during a sensing window, P_s , and corresponding expressions for P'_d and P'_f derived in Chapter 3 assumed the probability of higher order PU state switching was negligible and if the PU switched states during the sensing window, it would be in opposing states at the beginning and end of that sensing window. That is, if the PU was ON at the beginning of a sensing window and the PU switched during that sensing window, the PU was then assumed to be OFF at the end of the sensing window and vice versa. The case where the PU switched more than once and was in the same state at the beginning and end of the sensing window was not considered. The work presented in this chapter addresses this case.

Again, the dynamic scenario described in Chapter 2 and illustrated in Figure 6 is assumed. Therefore, the PU may switch at any time, independent of the SU sensing window. Furthermore, if during a sensing window a PU is both ON and OFF the definitions of the probabilities of detection and false alarm given in Chapter 2, equations (16) and (17), are no longer valid. Therefore the expressions are redefined as in Chapter 3, equations (30) and (31) which are repeated here for convenience.

$$P'_d(N) = \Pr(Y > \lambda | H_1 \text{ is true at time instant } N) \quad (36)$$

$$P'_f(N) = \Pr(Y > \lambda | H_0 \text{ is true at time instant } N). \quad (37)$$

Using these definitions for P'_d and P'_f one could consider all potential variants of PU activity within a sensing window. Specifically, the PU may switch states anywhere between zero and $N - 1$ times during a sensing window. Figure 18 illustrates various PU activity scenarios with respect to a single sensing window.

4.1 PROBABILITY OF VOLATILE PRIMARY USER STATE SWITCH

The scenarios in Figure 18 are subdivided into two groups. Those scenarios on the left result in the PU being ON at the end of the sensing window while the scenarios on the right

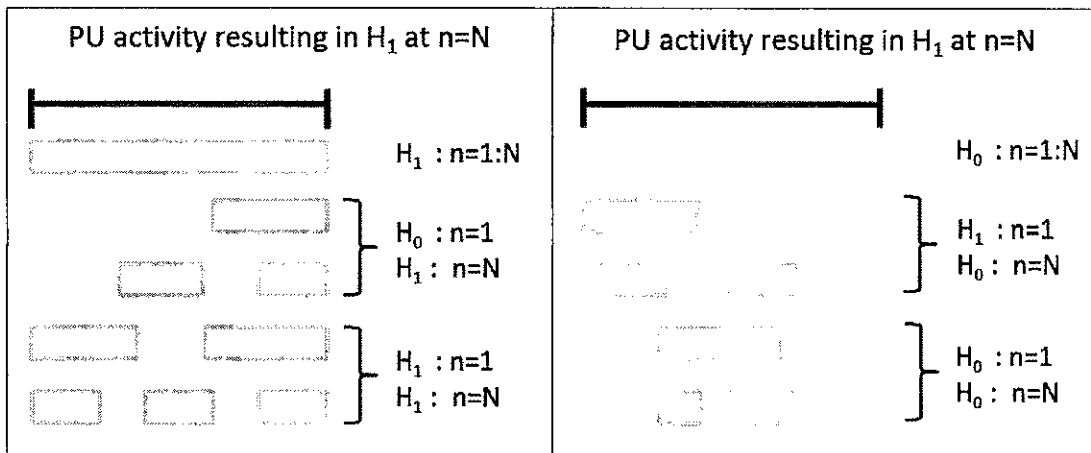


Figure 18: Higher order PU switching during sensing window.

result in the PU being OFF at the end of the sensing window. Focusing on the scenarios on the left, the scenarios are organized into three cases. In the first case the PU is active the entire sensing window. The second case is representative of the PU being OFF at the beginning of the sensing window then switches states an odd number of times during the sensing window. This results in the PU being ON at the end of the sensing window. Finally, in the third case the PU is ON at the beginning of the sensing window then switches states an even number of times during the sensing window. In this case the PU is ON at both the beginning and end of the sensing window. The scenarios resulting in the PU being OFF at the end of the sensing window can be described in a similar manner. In total, there are six distinct cases versus the four cases described in Chapter 3. The probabilities of each of these cases occurring is: \bar{P}_{ON} , $\bar{P}_{OFF \rightarrow ON}$, $\bar{P}_{ON \rightarrow ON}$, \bar{P}_{OFF} , $\bar{P}_{ON \rightarrow OFF}$, and $\bar{P}_{OFF \rightarrow OFF}$. The overbar is meant to create a distinction between these probabilities and those presented in Chapter 3.

Like the four cases described in Chapter 3, the six cases in Figure 18 are mutually exclusive, thus their probabilities add to unity. Further, it is again noted that each case is dependent on both the state of the PU at the beginning of the sensing window and the PU activity during the sensing window.

Using the PU activity described in Chapter 2 and illustrated in Figure 6, the duration of a spectrum hole and that of a PU transmission, relative to the SU discrete samples, are

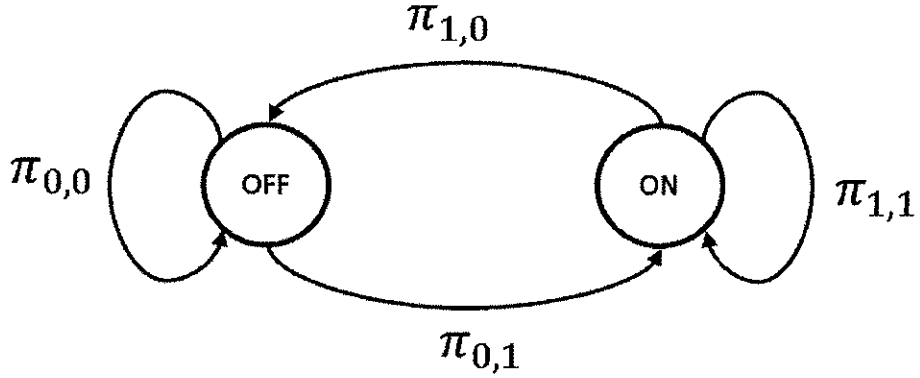


Figure 19: Markov chain representation of PU activity.

exponentially distributed with respective means μ and τ . Thus the probability of the PU being present (ON) at the beginning of a sensing window is provided in equation (23), while the probability of the PU being absent (OFF) is provided in equation (24). These expressions are repeated here for convenience:

$$p_p = \frac{\tau}{\tau + \mu} \quad (38)$$

$$p_a = \frac{\mu}{\tau + \mu}. \quad (39)$$

The PU activity during the sensing window captures the PU switching behavior in N samples. In order to capture higher order switching behavior, the analysis must deviate from that presented in Chapter 3. Thus, the PU activity is described with the two-state Markov chain in Figure 19. In this figure, $\pi_{i,j}$ represents the probabilities of a PU, which is in state i in sample n , switching to state j in sample $n + 1$. To simplify notation, the state when the PU is OFF is designated by the subscript 0, while the state when the PU is ON is designated by the subscript 1. The switching probabilities are defined in the one-step transition matrix:

$$\Pi = \begin{bmatrix} \pi_{0,0} & \pi_{0,1} \\ \pi_{1,0} & \pi_{1,1} \end{bmatrix}. \quad (40)$$

Given that the spectrum hole and PU transmission are exponentially distributed with respective means μ and τ , the one-step transition matrix is:

$$\Pi = \begin{bmatrix} (e^{-1/\mu}) & (1 - e^{-1/\mu}) \\ (1 - e^{-1/\tau}) & (e^{-1/\tau}) \end{bmatrix}. \quad (41)$$

Because the Markov chain in Figure 19 is homogeneous, the N -step transition matrix is Π^N , where $\pi_{i,j}^{(N)}$ is the (i, j) th entry of Π^N . Furthermore, $\pi_{i,j}^{(N)}$ represents the probabilities of a PU, which is in state i in sample n , being in state j in sample $n + N$. It is critical to note the distinction between $\pi_{i,j}^N$ and $\pi_{i,j}^{(N)}$. The prior is an individual probability raised to the N th power while the latter is an element of a matrix which was raised to the N th power.

As like all homogenous Markov chains, the system is completely defined by the one-step transition matrix and the initial probability distribution [27]. In this case the initial probability distributions are p_p and p_a . Therefore, it is possible to define the probability of each of the six sensing window cases occurring. \bar{P}_{ON} , represents the probability of the PU being ON for the duration of a sensing window. It is the joint probability of the PU being present and the probability the PU does not switch during within N samples

$$\bar{P}_{ON} = p_p \cdot \pi_{1,1}^N = p_p \cdot e^{-N/\tau}. \quad (42)$$

As would be expected, the equation for \bar{P}_{ON} is equal to (25) for P_{ON} in Chapter 3. Similarly, the probability that the PU remains OFF for the duration of a sensing window is the joint probability of the PU being absent and the PU not switching within N samples

$$\bar{P}_{OFF} = p_a \cdot \pi_{0,0}^N = p_a \cdot e^{-N/\mu}. \quad (43)$$

This is equal to (27) for P_{OFF} in Chapter 3.

The four remaining cases utilize the individual entries in the N -step transition matrix. The probability of the PU switching from ON to OFF over a sensing window is the joint probability of the PU being present and the PU switching an odd number of times within N samples resulting in the PU being OFF at the end of the sensing window

$$\bar{P}_{ON \rightarrow OFF} = p_p \cdot \pi_{1,0}^{(N)}. \quad (44)$$

It is important to note that $\bar{P}_{ON \rightarrow OFF}$ is not equivalent to $P_{ON \rightarrow OFF}$ as given in (26) in Chapter 3.

The probability of the PU switching from OFF to ON over a sensing window is the joint probability of the PU being absent and the PU switching an odd number of times within N samples resulting in the PU being ON at the end of the sensing window

$$\bar{P}_{OFF \rightarrow ON} = p_a \cdot \pi_{0,1}^{(N)}. \quad (45)$$

Again, $\bar{P}_{OFF \rightarrow ON}$ is not equivalent to $P_{OFF \rightarrow ON}$ in Chapter 3 equation (28). However, while not immediately apparent the expressions $\bar{P}_{OFF \rightarrow ON}$ and $\bar{P}_{ON \rightarrow OFF}$ are equivalent. Based on knowledge of the Markov chain from which these expressions were derived, it does stand to reason that the probability of the PU being ON at $n = 1$ and OFF at $n = N$ is the same as the probability of the PU being OFF at $n = 1$ and ON at $n = N$.

The probability of the PU switching from ON to ON over a sensing window is the joint probability of the PU being present and the PU switching an even number of times within N samples resulting in the PU being ON at the end of the sensing window

$$\bar{P}_{ON \rightarrow ON} = p_p \cdot (\pi_{1,1}^{(N)} - \pi_{1,1}^N). \quad (46)$$

In this case $\pi_{1,1}^{(N)}$ represents the probability of the PU which was ON at the beginning of the sampling window is also ON at the end of the sampling window. In order to distinguish between the case where the PU switched states an even number of times and the case where the PU did not switch at all, $\pi_{1,1}^N$ was subtracted from $\pi_{1,1}^{(N)}$.

The probability of the PU switching from OFF to OFF over a sensing window is derived in a similar manner as the expression for $\bar{P}_{ON \rightarrow ON}$. This is the joint probability of the PU being absent and the PU switching an even number of times within N samples resulting in the PU being OFF at the end of the sensing window

$$\bar{P}_{OFF \rightarrow OFF} = p_a \cdot (\pi_{0,0}^{(N)} - \pi_{1,1}^N). \quad (47)$$

The total probability of the PU switching states during a sensing period \bar{P}_s is the sum of the last four cases presented

$$\bar{P}_s = \bar{P}_{ON \rightarrow OFF} + \bar{P}_{OFF \rightarrow ON} + \bar{P}_{ON \rightarrow ON} + \bar{P}_{OFF \rightarrow OFF}. \quad (48)$$

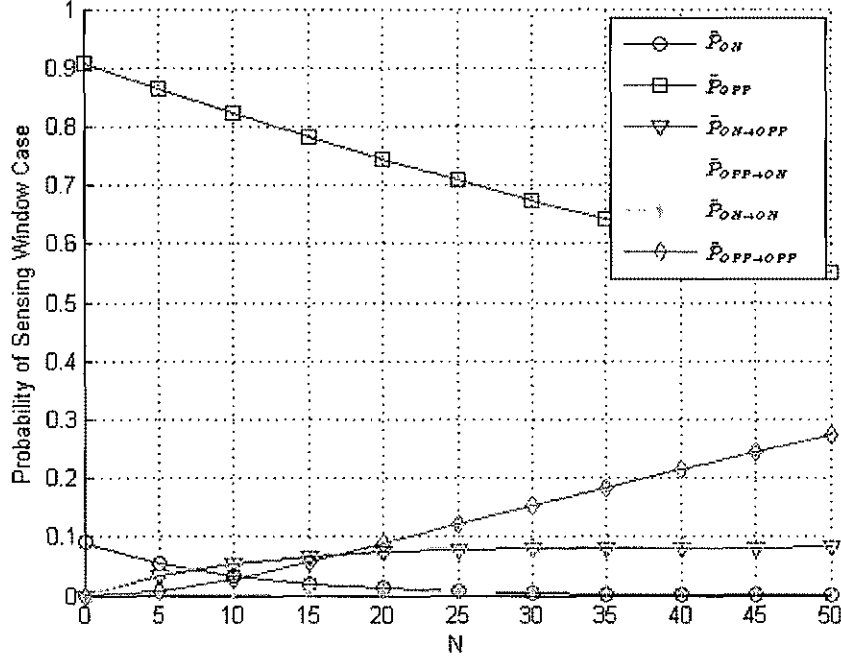


Figure 20: Volatile PU sensing window probabilities versus N for $\mu=100$, $\tau=10$.

It is of interest that for any given set of input values μ , τ , and N , the value of \bar{P}_s is equivalent to (29) for P_s in Chapter 4. This equivalency is due to the following identities:

$$P_{ON \rightarrow OFF} = \bar{P}_{ON \rightarrow OFF} + \bar{P}_{ON \rightarrow ON} \quad (49)$$

$$P_{OFF \rightarrow ON} = \bar{P}_{OFF \rightarrow ON} + \bar{P}_{OFF \rightarrow OFF}. \quad (50)$$

Because \bar{P}_s is equivalent to P_s , Figure 8 in Chapter 3 and observations made from this figure not only represents P_s , but \bar{P}_s as well.

Figures 20, 21, and 22 provide the individual switching window probabilities versus N for the three PU activity levels simulated in Chapter 3: $\tau = 10$ and $\mu = 100$; $\tau = 100$ and $\mu = 100$; and $\tau = 200$ and $\mu = 100$. In all three figures the sum of the sensing window probabilities adds to unity for each value of N . Additionally it can be seen in all three figures that $\bar{P}_{OFF \rightarrow ON}$ and $\bar{P}_{ON \rightarrow OFF}$ are equivalent as stated previously. Examining the figures independently reveals further items of interest concerning the three PU activity levels.

Figure 20 reveals that with a sensing window larger than $N = 17$ samples, the value of

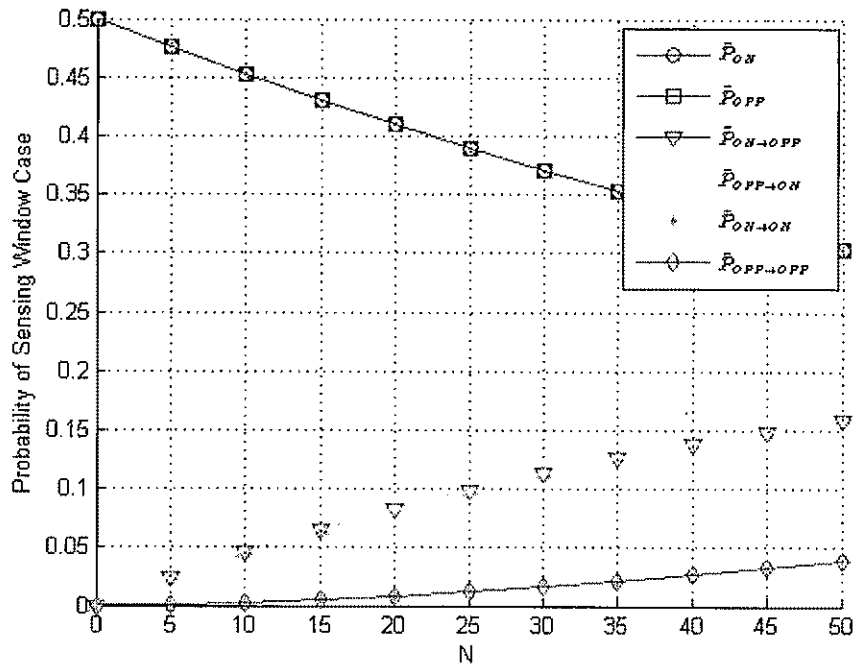


Figure 21: Volatile PU sensing window probabilities versus N for $\mu=100$, $\tau=100$.

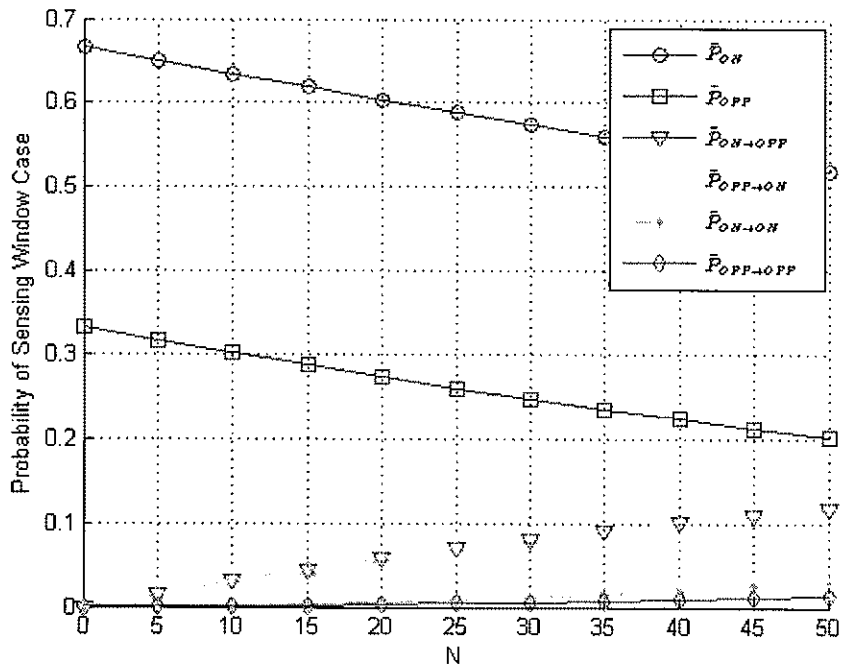


Figure 22: Volatile PU sensing window probabilities versus N for $\mu=100$, $\tau=200$.

$\bar{P}_{OFF \rightarrow OFF}$ exceeds all other switching window probabilities except \bar{P}_{OFF} . The relatively high probability of $\bar{P}_{OFF \rightarrow OFF}$ is of interest due to the fact that the analysis provided in Chapter 3 assumed the probability of higher order switching was negligible. Because $\bar{P}_{OFF \rightarrow OFF}$ represents the case when the PU switches at least twice during the sensing window, this assumption is clearly not valid for the PU activity level $\tau = 10$ and $\mu = 100$.

As one would expect, equal values of μ and τ result in \bar{P}_{ON} and \bar{P}_{OFF} being equal as well as $\bar{P}_{ON \rightarrow ON}$ and $\bar{P}_{OFF \rightarrow OFF}$ being equal. This is shown in Figure 21. While $\bar{P}_{OFF \rightarrow ON}$ and $\bar{P}_{ON \rightarrow OFF}$ are also equivalent in Figure 21, this is again true for all values of μ and τ and not just the case where μ equals τ .

Additionally, Figure 21 reveals that $\bar{P}_{ON \rightarrow ON}$ and $\bar{P}_{OFF \rightarrow OFF}$ each are relatively small and for smaller values of N the assumptions made in Chapter 3 concerning higher order PU switching are reasonable for this PU activity level. Figure 22 again shows that that $\bar{P}_{ON \rightarrow ON}$ and $\bar{P}_{OFF \rightarrow OFF}$ each are relatively small and again for smaller values of N the assumptions made in Chapter 3 are reasonable for the PU activity level.

4.2 VOLATILE PRIMARY USER IMPACT ON SENSING PERFORMANCE

To determine the expression of the probability of detection, as defined by equation (36), that includes the impact of higher order PU state switching, one should consider three case: the PU is ON for the entire sensing window, the PU is OFF at the beginning of the sensing window, then switches an odd number of times and is ON at the end of the sensing window, and the PU is ON at the beginning of the sensing window then switches an even number of times and is ON at the end of the sensing window. These cases are illustrated by the sensing windows on the left side of Figure 18 and represented by the probabilities \bar{P}_{ON} in equation (42), $\bar{P}_{OFF \rightarrow ON}$ in equation (45), and $\bar{P}_{ON \rightarrow ON}$ in equation (46).

When the PU state is ON for the entire sensing window the probability of detection is $P_d(N)$ as outlined in Chapter 2, equation (17) in the case of AWGN channels or (21) for fading channels. If, however, the PU state switches during the sensing window from either OFF to ON or ON to ON, the probability of detection $P_{ds}(N)$ is given by equation (32) in Chapter 3. Thus, the expression of the probability of detection that considers higher order

PU state switching is:

$$\begin{aligned}\bar{P}_d(N) &= \frac{\bar{P}_{ON} \cdot P_d(N) + (\bar{P}_{OFF \rightarrow ON} + \bar{P}_{ON \rightarrow ON}) \cdot P_{ds}(N)}{\bar{P}_{ON} + \bar{P}_{OFF \rightarrow ON} + \bar{P}_{ON \rightarrow ON}} \\ &= \frac{\bar{P}_{ON} \cdot P_d(N) + (\bar{P}_{OFF \rightarrow ON} + \bar{P}_{ON \rightarrow ON}) \cdot P_{ds}(N)}{p_p}.\end{aligned}\quad (51)$$

The simplification of the denominator is possible due to the fact that the probabilities were derived from a homogenous Markov chain [27].

To determine the expression of the probability of false alarm as defined by (37) which takes into account the impact of higher order PU state switch, a similar analysis is carried out. In this situation one should consider the case where the PU is OFF for the entire sensing window, the case where the PU switches from ON to OFF during the sensing window, and the case where the PU switches from OFF to OFF during the sensing window. When the PU state is OFF for the entire sensing window the probability of false alarm is $P_f(N)$ as outlined in Chapter 2 and is given by equation (16). When the PU state switches either from ON to OFF or OFF to OFF the probability of false alarm P_{fs} is as given in Chapter 3 equation (34). Thus, the expression of the probability of false alarm that considers higher order PU state switching is

$$\begin{aligned}\bar{P}_f(N) &= \frac{\bar{P}_{OFF} \cdot P_f(N) + (\bar{P}_{ON \rightarrow OFF} + \bar{P}_{OFF \rightarrow OFF}) \cdot P_{fs}(N)}{\bar{P}_{OFF} + \bar{P}_{ON \rightarrow OFF} + \bar{P}_{OFF \rightarrow OFF}} \\ &= \frac{\bar{P}_{OFF} \cdot P_f(N) + (\bar{P}_{ON \rightarrow OFF} + \bar{P}_{OFF \rightarrow OFF}) \cdot P_{fs}(N)}{p_a}.\end{aligned}\quad (52)$$

4.3 VOLATILE PRIMARY USER NUMERICAL RESULTS

This section illustrates the performance of the proposed expressions for \bar{P}_d and \bar{P}_f in equations (51) and (52), respectively. Simulation results are presented and are compared to the theoretical ROC expressions from Chapter 2, which do not consider P_s , and the proposed theoretical ROC expressions from this chapter, which consider higher order PU switching.

The simulation set up was as described in Chapter 3. Again, AWGN and Rayleigh fading channels were analyzed. The theoretical ROC which considers \bar{P}_s used the expressions

for \bar{P}_d in equation (51) and \bar{P}_f in equation (52), where P_d and P_f used in the expressions are respectively (22) and (19) for Rayleigh fading channels and respectively (20) and (19) for AWGN channels. The theoretical ROC which does not consider P_s uses equations (22) and (19) for Rayleigh channels and (20) and (19) for AWGN channels.

The first simulation used the PU activity level $\tau = 10$ and $\mu = 100$ and $\gamma = -5$ dB with results in Figure 23. While the second simulation used the same PU activity level as the first but γ was increased to 0 dB. The results of the second simulation are provided in Figure 24. In both cases, the simulated results were a better match to the theoretical ROC which considered \bar{P}_s than the ROC which did not. However, the theoretical expressions derived in this chapter did not perform any better than those derived in Chapter 3. Given the volatile PU activity level in the first two simulations this was unexpected.

The next two simulations considered the PU activity level $\tau = 100$ and $\mu = 100$ first with a $\gamma = -5$ dB with results in Figure 25 then with $\gamma = 0$ dB with results in Figure 26. The final two simulations considered a PU activity level $\tau = 200$ and $\mu = 100$. This activity level was first simulated with $\gamma = -5$ dB with results in Figure 27 then with $\gamma = 0$ dB with results in Figure 28. In all four simulations the simulated results were close to the theoretical ROC which considered \bar{P}_s . Furthermore, like the first two simulations the theoretical expressions derived in this chapter did not perform any better than those derived in Chapter 3. However, with the less dynamic PU activity levels this was expected.

In this chapter, the impact of PU higher order PU switching on the overall sensing performance of an energy detector was examined. The simulation results indicate that in the context of the dynamic scenario described in Chapter 2 the proposed expressions for \bar{P}_d and \bar{P}_f within this chapter are a better analytical measure of performance than the expressions for P_d and P_f within Chapter 2 but do not appear to outperform the analytic expressions of P'_d and P'_f proposed in Chapter 3.

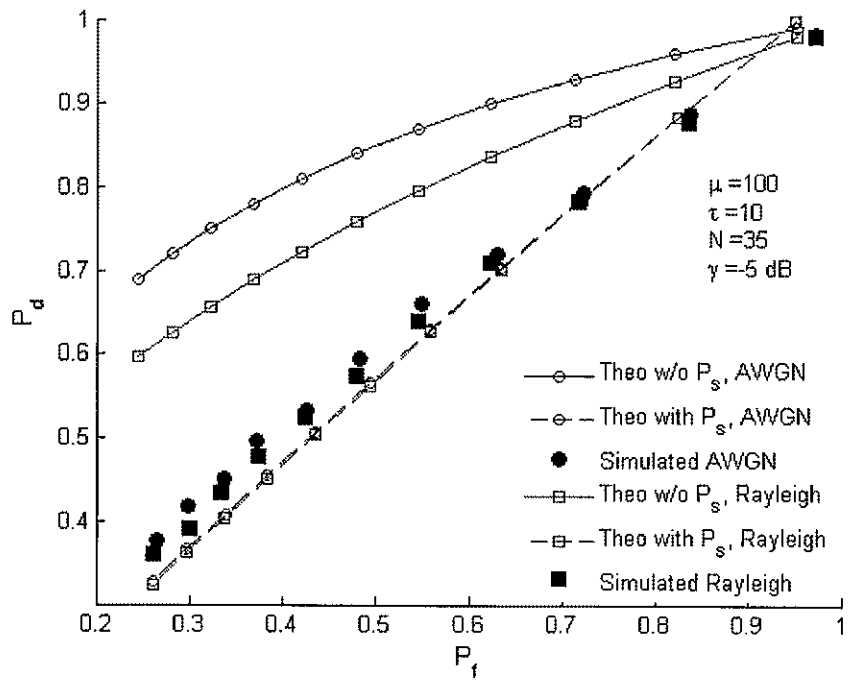


Figure 23: Volatile PU ROCs for $\mu=100$, $\tau=10$, and $\gamma = -5$ dB.

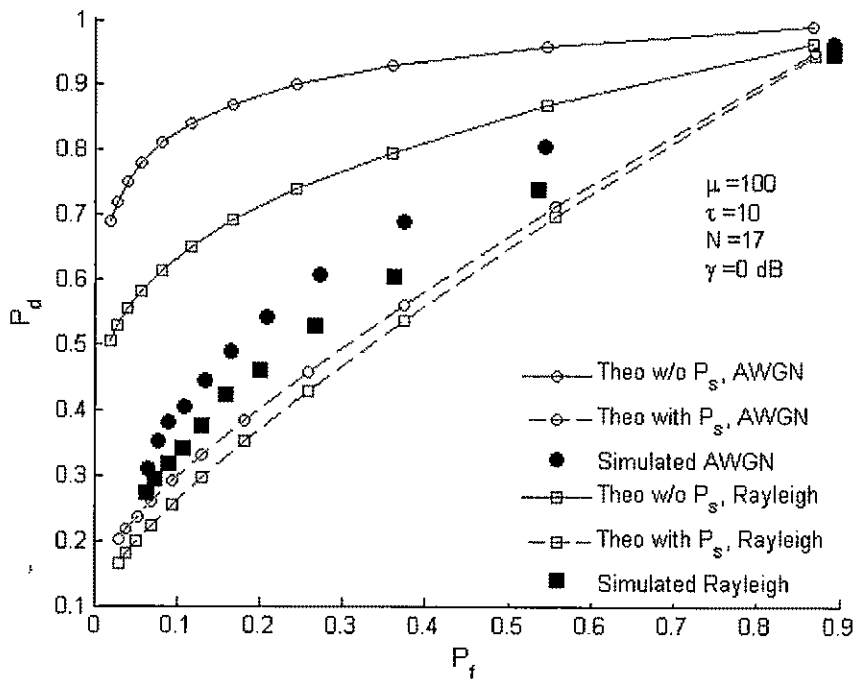


Figure 24: Volatile PU ROCs for $\mu=100$, $\tau=10$, and $\gamma = 0$ dB.

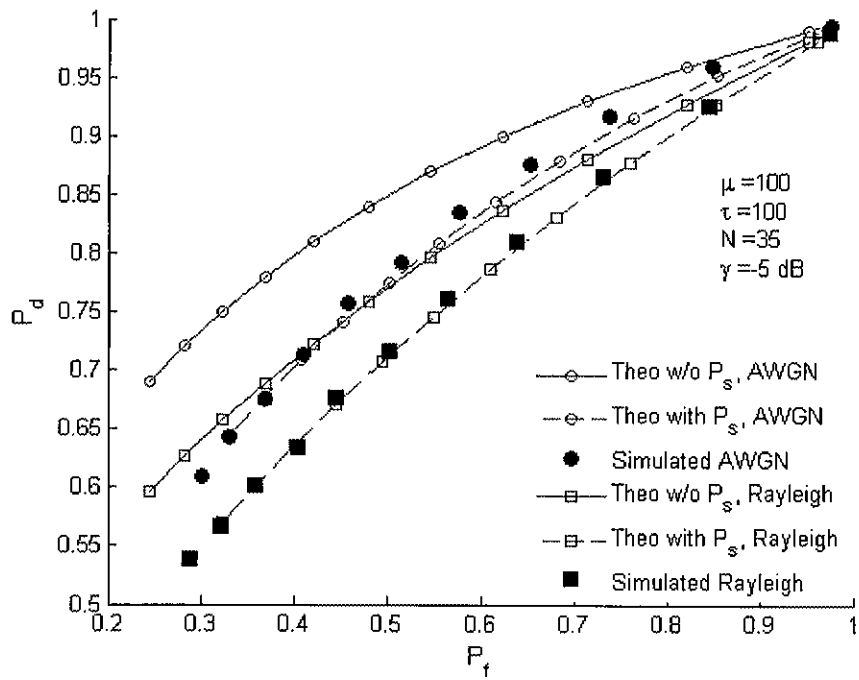


Figure 25: Volatile PU ROCs for $\mu=100$, $\tau=100$, and $\gamma = -5$ dB.

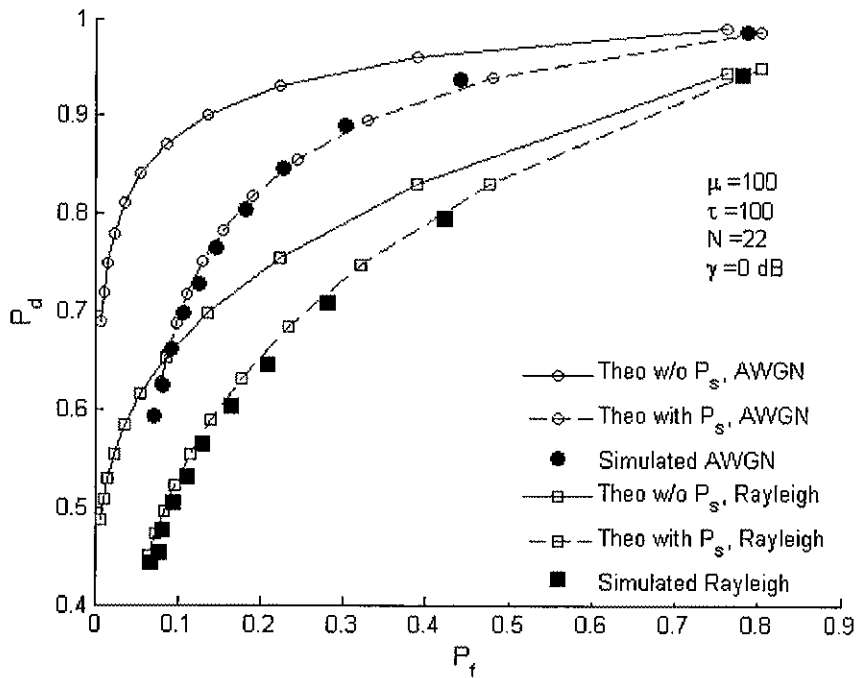


Figure 26: Volatile PU ROCs for $\mu=100$, $\tau=100$, and $\gamma = 0$ dB.

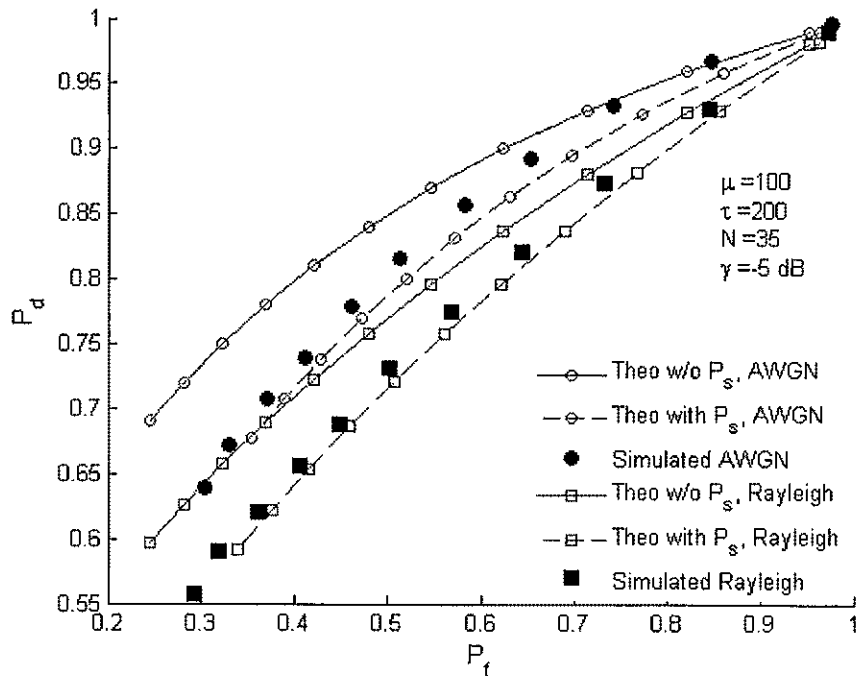


Figure 27: Volatile PU ROCs for $\mu=100$, $\tau=200$, and $\gamma = -5$ dB.

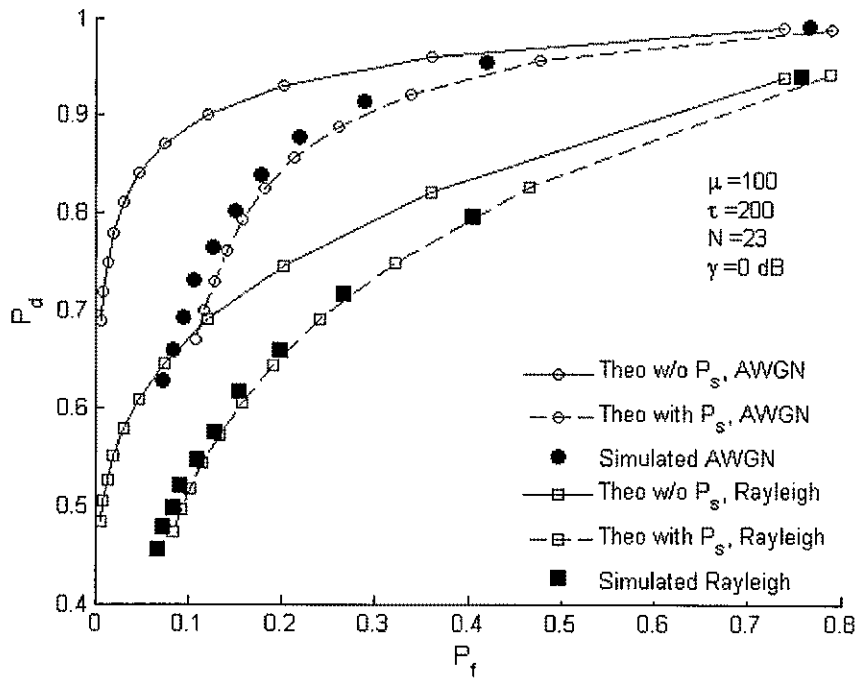


Figure 28: Volatile PU ROCs for $\mu=100$, $\tau=100$, and $\gamma = 0$ dB.

CHAPTER 5

CONCLUSIONS

CR is an emerging technology that has promising potential to enable the sharing of spectrum in order to meet ever growing spectral demands. Over the past decade there has been a great amount of research in the area of CR, however the technology is still in its early stages and there are several technical issues to research. This thesis explored one of those issues related to reliable spectrum sensing.

CR is a broad technology which is comprised of several technical fields, one of which is spectrum sensing. Within CR systems, spectrum sensing is done by the SU in order to opportunistically access the spectrum. There are multiple spectrum sensing technologies; this thesis focused on energy-based spectrum sensing.

The contributions of this thesis are analytic expressions for performance of energy detection in a dynamic PU scenario. In the dynamic PU scenario, the SU was unaware of the PU waveform or transmission timing. Therefore, the PU switched states during the SU sensing window with probability P_s . This thesis provided two alternative approaches for calculating P_s and derived corresponding analytical expressions for P_d and P_f which considered P_s . The first set of analytic expressions for energy detection assumed the PU only switched once during the SU sensing window. In general the numerical results supported the derived analytic expressions, with the exception of a single case with a volatile PU and a smaller sensing window. The second set of analytic expression removed the assumption that the PU would only switch once during a sensing window such that the case of a more volatile PU would be considered. Unexpectedly, this expression did not do a better job of matching the results from the simulation with a volatile PU and a smaller sensing window. Examining the reason for these unexpected results will be included in short-term future research.

As noted, CR is still in its early stages with significant opportunities for future research. In the short-term this work can be extended. This work considered a single PU with activity

that was exponentially distributed. The derived expressions should be extended to consider general cases of PU activity. In particular PU activity distributions that are not memoryless should be considered as well as a multiple PU scenario. Long-term research includes the exploration of spectrum sensing using automatic modulation classification, a signal processing technique to estimate the modulation scheme of unknown noisy signals based on multiple hypotheses.

REFERENCES

- [1] Federal Communications Commission, “Notice of Proposed Rule Making and Order: Facilitating Opportunities for Flexible, Efficient, and Reliable Spectrum Use Employing Cognitive Radio Technologies,” *ET Docket*, February 2005.
- [2] Federal Communications Commission, “Report of the Spectrum Efficiency Working Groups,” *ET Docket*, November 2002.
- [3] Presidents Council of Advisors on Science and Technology, “Realizing the Full Potential of Government-held Spectrum to Spur Economic Growth,” *ET Docket*, July 2012.
- [4] W. Krenik, A. M. Wyglinsky, and L. Doyle, “Cognitive Radios for Dynamic Spectrum Access,” *IEEE Communications*, vol. 45, pp. 64–65, May 2007.
- [5] S. Haykin, J. Reed, G. Li, and M. Shafi, “Scanning the Issue,” *Proceedings of the IEEE*, vol. 97, pp. 608–611, April 2009.
- [6] J. Mitola and G. Q. Maguire, “Cognitive Radio: Making Software Radios More Personal,” *IEEE Personal Communications*, vol. 6, pp. 13–182, August 1999.
- [7] T. Yucek and H. Arslan, “A Survey of Spectrum Sensing Algorithms for Cognitive Radio Applications,” *IEEE Communications Surveys and Tutorials*, vol. 11, pp. 116–130, 2009.
- [8] H. Urkowitz, “Energy Detection of Unknown Deterministic Signals,” *Proceedings of the IEEE*, vol. 55, pp. 523–531, April 1967.
- [9] H. Tang, “Some Physical Layer Issues of Wide-band Cognitive Radio Systems,” in *Proceedings of 2005 DySPAN Conference*, pp. 151–159, November 2005.
- [10] W. Gardner, “Exploitation of Spectral Redundancy in Cyclostationary Signals,” *IEEE Signal Processing*, vol. 8, pp. 14–36, April 1991.

- [11] R. Tandra and A. Sahai, "Fundamental Limits on Detection in Low SNR under Noise Uncertainty," in *Proceeding of 2005 International Conference on Wireless Networks, Communications and Mobile Computing*, vol. 1, pp. 464–469, June 2005.
- [12] E. Axell, G. Leus, E. G. Larsson, and H. V. Poor, "Spectrum Sensing for Cognitive Radio: State-of-the-Art and Recent Advances," *IEEE Signal Processing Magazine*, vol. 29, pp. 101–116, May 2012.
- [13] F. Digham, M.-S. Alouini, and M. Simon, "On the Energy Detection of Unknown Signals over Fading Channels," in *Proceeding of 2003 IEEE International Conference on Communications*, vol. 5, pp. 3575–579, May 2003.
- [14] Y. C. Liang, Y. Zeng, E. C. Peh, and A. T. Hoang, "Sensing-Throughput Tradeoff for Cognitive Radio Networks," *IEEE Transactions on Wireless Communications*, vol. 7, pp. 1326–1337, April 2008.
- [15] D. Treeumnuk and D. Popescu, "Adaptive Sensing for Increased Spectrum Utilization in Dynamic Cognitive Radio Systems," in *Proceeding of 2012 IEEE Radio and Wireless Symposium*, pp. 319–322, January 2012.
- [16] R. Tandra, A. Sahai, and M. Mishra, "What is a Spectrum Hole and What Does it Take to Recognize One?," *Proceedings of IEEE*, vol. 97, pp. 824–848, May 2009.
- [17] D. Treeumnuk and D. Popescu, "Energy Detector with Adaptive Sensing Window for Improved Spectrum Utilization in Dynamic Cognitive Radio Systems," in *Proceeding of 2012 IEEE International Conference on Communications*, pp. 1528–1532, June 2012.
- [18] D. Treeumnuk and D. Popescu, "Using Hidden Markov Models to Enable Performance Awareness and Noise Variance Estimation for Energy Detection in Cognitive Radio," in *Proceeding of 2012 Conference on Information Sciences and Systems*, March 2012.

- [19] R. Fantacci and A. Tani, "Performance Evaluation of a Spectrum-Sensing Technique for Cognitive Radio Applications in B-VHF Communication Systems," *IEEE Transactions on Vehicular Technology*, vol. 58, pp. 1722–1730, May 2009.
- [20] J. E. Salt and H. H. Nguyen, "Performance Prediction for Energy Detection of Unknown Signals," *IEEE Transactions on Vehicular Technology*, vol. 57, pp. 3900–3904, November 2008.
- [21] Y. Zou, Y.-D. Yao, and B. Zheng, "Outage Probability Analysis of Cognitive Transmissions: Impact of Spectrum Sensing Overhead," *IEEE Transactions on Wireless Communications*, vol. 9, pp. 2676–2688, August 2010.
- [22] F. Penna and R. Garello, "Detection of Discontinuous Signals for Cognitive Radio Applications," *IET Communications*, vol. 5, pp. 1453–1461, January 2011.
- [23] V. Kostylev, "Energy Detection of a Signal with Random Amplitude," in *Proceeding of 2002 IEEE International Conference on Communications*, vol. 3, pp. 1606–1610 vol.3.
- [24] F. F. Digham, M. S. Alouini, and M. K. Simon, "On the Energy Detection of Unknown Signals Over Fading Channels," *IEEE Transactions on Communications*, vol. 55, pp. 21–24, January 2007.
- [25] S. Geirhofer, L. Tong, and B. M. Sadler, "Cognitive Medium Access: Constraining Interference Based on Experimental Models," *IEEE Journal on Selected Areas in Communications*, vol. 26, pp. 95–105, January 2008.
- [26] F. Penna, C. Pastrone, M. Spirito, and R. Garello, "Energy Detection Spectrum Sensing with Discontinuous Primary User Signal," in *Proceeding of 2009 IEEE International Conference on Communications*, June 2009.
- [27] A. Papoulis and S. U. Pillai, *Probability, Random Variables, and Stochastic Processes*, McGraw Hill, 2002.

VITA

Sara L. MacDonald
Department of Electrical and Computer Engineering
Old Dominion University
Norfolk, VA 23529

Sara Lynn MacDonald was born [redacted] in Pierre, South Dakota. After graduating from Stevens High School, Rapid City, South Dakota, she went on to earn her Bachelor of Science in Electrical Engineering from South Dakota School of Mines and Technology in May 2000. While earning her bachelor's degree, Sara was inducted into Eta Kappa Nu and Tau Beta Pi engineering honor societies. After earning her bachelor's degree Sara was employed by Boeing in Anaheim, California, where her work focused on tactical communication systems. In 2009 she began working for MITRE in Hampton, Virginia, where she is currently employed. In Spring 2010 she enrolled at Old Dominion University, earning her Master of Science in Electrical and Computer Engineering in May 2013.